horticulturae

MDPI

Article

Establishment of a Protocol for the Characterization of Secreted Biomolecules in Somatic Embryogenic Cultures of *Olea europaea* L.

Rita Pires [1], Lénia Rodrigues [1], Fátima Milhano Santos [2], Iola F. Duarte [3], Sergio Ciordia [4], Augusto Peixe [5] and Hélia Cardoso [5,*]

[1] MED—Mediterranean Institute for Agriculture, Environment and Development & CHANGE—Global Change and Sustainability Institute, Instituto de Investigação e Formação Avançada, Universidade de Évora, Pólo da Mitra, Ap. 94, 7002-554 Évora, Portugal; rnpires@uevora.pt (R.P.); liar@uevora.pt (L.R.)
[2] Health Research Institute-Fundación Jiménez Díaz University Hospital, Autonomous University of Madrid (IIS-FJD, UAM), 28040 Madrid, Spain; fatima.milhano@quironsalud.es
[3] Department of Chemistry, LAQV-REQUIMTE & CICECO—Aveiro Institute of Materials, University of Aveiro, Campus de Santiago, 3810-193 Aveiro, Portugal; ioladuarte@ua.pt
[4] Functional Proteomics Laboratory, National Center for Biotechnology (CNB-CSIC), Darwin 3, 28049 Madrid, Spain; sciordia@cnb.csic.es
[5] MED—Mediterranean Institute for Agriculture, Environment and Development & CHANGE—Global Change and Sustainability Institute, Escola de Ciências e Tecnologia, Universidade de Évora, Pólo da Mitra, Ap. 94, 7002-554 Évora, Portugal; apeixe@uevora.pt
* Correspondence: hcardoso@uevora.pt

Abstract: Somatic embryogenesis (SE) involves the formation of embryo-like structures from somatic cells without fertilization and is widely used for clonal propagation and genetic transformation. However, in olive (*Olea europaea* sp. *europaea*), SE remains challenging due to the recalcitrant behavior of adult tissues when used as initial explants. Bioactive molecules released into the culture medium (conditioned medium, CM) by embryogenic cultures have been identified as modulators of the SE response. However, their potential role in enhancing SE efficiency in olive and overcoming tissue recalcitrance remains largely unexplored. To investigate the role of these biomolecules in olive SE, a protocol was established using SE cultures of cv. 'Galega Vulgar'. Proteins and metabolites were separated by filtration, concentrated through lyophilization, and precipitated using three methods: Acetone, TCA/Acetone, and Methanol/Chloroform. The efficiency of these methods was evaluated through total protein quantification and via SDS-PAGE electrophoresis. LC-MS/MS was employed to analyze secretome composition using the TCA/Acetone precipitation method. Additionally, metabolite profiles were analyzed using ^{1}H NMR spectroscopy. The results led to the identification of 1096 (526 protein groups) *Olea europaea* proteins, including well-known SE biomarkers such as kinases and peroxidases. NMR spectroscopy identified several metabolites secreted into the medium or resulting from the metabolic activity of secreted enzymes, confirming the applicability of the procedure. Although extracting secreted biomolecules from the culture medium presents significant challenges, the protocol established in this study successfully enabled the isolation and identification of both proteins and metabolites, revealing a valuable workflow for future in-depth analyses of secreted biomolecules in olive SE.

Keywords: somatic embryogenesis; olive; conditioned medium; secretome; proteome; metabolome

Academic Editors: Rytis Rugienius, Audrius Sasnauskas and Akvile Virsile

Received: 24 January 2025
Revised: 28 February 2025
Accepted: 12 March 2025
Published: 19 March 2025

Citation: Pires, R.; Rodrigues, L.; Santos, F.M.; Duarte, I.F.; Ciordia, S.; Peixe, A.; Cardoso, H. Establishment of a Protocol for the Characterization of Secreted Biomolecules in Somatic Embryogenic Cultures of *Olea europaea* L. *Horticulturae* **2025**, *11*, 331. https://doi.org/10.3390/horticulturae11030331

1. Introduction

Somatic embryogenesis (SE) is a nonsexual propagation process regulated by complex mechanisms [1] that leads to the formation of structures resembling zygotic embryos. These structures arise from the dedifferentiation of somatic cells, which can generate a complete plant without fertilization. SE is widely used for clonal propagation in several plant species [2], providing suitable material for genetic transformation or to assist breeding programs following the manipulation of plant genome approaches (e.g., mutagenesis, and New Genomic Techniques) [3,4], synthetic seed production, and germplasm conservation [5]. However, the mechanisms by which a somatic cell develops into a whole plant are complex and remain poorly understood. The ability to shift cell development from the vegetative to the embryogenic pathway is restricted to a limited number of cells [6] and is regulated by complex endogenous and exogenous factors. Various factors have been tested to optimize SE protocols across different plant species. These include exogenous factors [7–10], such as the culture medium composition, type and concentration of plant growth regulators, and growth conditions, and endogenous factors, including genotype, explant type, and developmental stage [11–14]. In olive tree (*Olea europaea* subsp. *europaea*), the explant type is highlighted as one of the most limiting factors on the establishment of SE protocols (see [15]). In fact, most SE protocols developed for olive trees are based on juvenile tissues as initial explants, usually radicles and cotyledons of mature embryos [14,16–18]. However, this approach is less ideal for clonal propagation purposes due to the high genetic variability associated with zygotic tissues [14,17,19]. Obtaining SE from adult olive material remains challenging due to the recalcitrant behavior exhibited by most tested genotypes (see review in [13]). Exceptions are known for the cvs. 'Canino' and 'Moraiolo' [20] with the development of a double regeneration system through organogenesis, and for the cvs. 'Chetoui' [21], 'Dahbia' [11], 'Picual' [22], and 'Moroccan Picholine' [10].

Despite the availability of some SE protocols using olive adult plant tissues, those protocols are not routinely and widely used in olive propagation due to the high genotype dependency of SE response (see [15] for details), a factor particularly critical, as even closely related genotypes can exhibit recalcitrance behavior when using a highly efficient protocol established for a distinct genotype [12,17].

In this context, discovering the molecular mechanism controlling SE efficiency is essential to overcome recalcitrance in olive. An important factor reported to affect SE in different plants species, but which has received little attention from the scientific community and has not been considered in any studies on olive trees, is the release of bioactive molecules by explants into liquid culture medium that could be used to modulate SE efficiency. This approach is based on the establishment of nurse-cell cultures, which means highly efficient liquid embryogenic cultures from which the culture medium is collected (commonly referred to as conditioned medium, CM) and further used to establish SE cultures using recalcitrant plant material [2]. The influence of CM composition derived from nurse-cell culture systems on inducing or modulating the SE response efficiency has long been observed [2–26]. The use of this approach to modulate the SE response in recalcitrant genotypes has been particularly explored in gymnosperms. Dyachok et al. [27] reported that extracts of media conditioned by embryogenic cultures of *Picea abies* stimulate the development of pro-embryogenic masses, suggesting that an endogenous lipophilic chitin oligosaccharide acts as a signal molecule in this process. Recently, Pernis et al. [28] reported proteomic data on the secretome of *Pinus nigra* cell lines with contrasting embryogenic capacity, revealing that cell wall-related and carbohydrate-acting proteins were the most differentially accumulated in the CM, with peroxidases (POXs), extensin, α-amylase, and basic secretory protease (BSP) being more abundant in highly embryogenic lines.

The effectiveness of the use of the CM has stimulated research aiming to identify the biomolecules that could play the crucial role in cell-to-cell communication and consequently induce/modulate SE response [29]. Within the secreted molecules that have been demonstrated to induce, or modulate, the SE response, there are extracellular proteins, growth regulators, vitamins, lipophilic molecules, and secondary metabolites [30–32]. Some studies have analyzed the CM from embryogenic cultures to identify proteins and metabolites that could serve as biomarkers of SE efficiency [28,29,33] or as modulators by supplementing the culture medium with these biomolecules [34–37]. These investigations have demonstrated that specific extracellular proteins play a significant role in the differentiation and morphogenesis of somatic cells [29], functioning as either promoters or inhibitors of SE [38]. For example, Arabinogalactan proteins (AGPs), a family of extracellular proteoglycans in plants, are implicated in many aspects of growth and development and have been directly linked to SE efficiency in *Areca catechu* [39]. Other proteins comprising the secretome and proposed as biomarkers of SE efficiency in different plant species were the Germin-like proteins identified in *P. balfouriana* [40], the Heat shock proteins in *Sorghum bicolor* [33], and the Chitinases [41], POXs, and α-amylases in *P. nigra* [28]. Kreuger and van Holst [42] showed that adding exogenous AGPs to the culture medium re-induced embryogenic competence in a non-embryogenic cell line in *Daucus carota*. Later studies confirmed AGPs as SE inducers, promoting somatic embryo formation. Similarly, Ben-Amar et al. [43] found that exogenous chitinases boosted cell population and embryogenic cell multiplication in *Cucurbita pepo* cultures.

Studies focused on the identification and quantification of a wide range of biomolecules require accurate and high sensitive analytical platforms. As reviewed by Tchorbadjieva [44], gel-based techniques like sodium dodecyl sulfate–polyacrylamide gel electrophoresis (SDS-PAGE) and two-dimensional polyacrylamide electrophoresis (2DE), occasionally complemented with immunoblotting, were among the initial approaches employed for fractionating and analyzing proteins secreted during SE. However, the development of advanced proteomic platforms, such as nano-liquid chromatography coupled to mass spectrometry (nLC-MS/MS), enables the detection and quantification of hundreds to thousands of proteins, including low-abundant proteins comprising the CM [45], making it the most appropriate approach. Similarly, many other biomolecules have been identified as comprising the CM. From the metabolites that compose the extracellular metabolome of CM, it was reported that caffeine and chlorogenic acid are the most abundant, while hydroxybenzoic acid and trans-cinnamic acid, found in very low concentrations, negatively influence SE in *Coffea canephora* [29]. In another study in *Solanum betaceum* [46], anthranilic acid was shown to inhibit the growth of established *calli* during SE. The results suggested a correlation between some secondary metabolites and dedifferentiation rates during induction, with a tendency to inhibit *callus* growth, likely due to metabolic effects.

Various techniques have been used for identifying and quantifying those metabolites that could be involved in modulating SE response. Nuclear Magnetic Resonance (NMR)-based metabolomics offers a non-targeted approach, providing a quantitative profile of metabolites within a sample. Unlike other techniques, such as chromatography (e.g., MS, UV, electrochemical), NMR does not require the prior separation of metabolites before detection [47], making it an alternative for investigating the metabolome composition of the CM matrix. In *P. glauca*, Dowlatabadi et al. [48] used 1D 1H NMR spectroscopy to identify intracellular metabolites such as γ-aminobutyric acid, malate, 5-oxoproline, isoleucine, valine, branched-chain keto acids, short-chain keto acids, glutamine, and phenylalanine. Their findings highlighted that the embryonic development of white spruce cells can be effectively monitored, with key metabolites implicated in developmental processes, thus providing insights into the optimization of SE developmental conditions.

Supported by prior knowledge of the importance of the CM as an inducer or modulator of the SE response, our objective was to establish a protocol for the simultaneous isolation of the secretome and extracellular metabolome to identify and quantify the proteins and metabolites comprising the CM matrix from olive somatic embryogenic cultures. This approach will support future research aimed at identifying the molecular mechanisms governing the SE response in this species, contributing to the optimization of protocols for recalcitrant genotypes.

2. Materials and Methods

2.1. Plant Material

Olea europaea subsp. *europaea* L. cv. 'Galega Vulgar' embryogenic lines were previously established using radicles and cotyledons of zygotic embryos cultivated in Agar-gelled Olive Medium culture (OMc) [49] supplemented with 2.5 µM 6-dimethylallylamino-purine (2iP), 25 µM indole-3-butyric acid (IBA) [50] and 6 g L^{-1} Agar-Powder (VWR, Lisbon, Portugal). Cultures at the induction phase were kept at 25 °C and 0 h photoperiod for 21 days. Developed *calli* were further transferred to an Agar-gelled expression OMc medium (6 g L^{-1} Agar-Powder, VWR, Lisbon, Portugal) devoid of plant growth regulators to promote embryo differentiation. Cultures were maintained for 30 days under the same conditions of temperature and photoperiod as those used in the induction phase. Embryogenic *calli* and somatic embryos of a selected high embryogenic line were transferred to an Agar-gelled Embryogenesis Cyclic Olive (ECO) culture medium (6 g L^{-1} Agar-Powder, VWR, Lisbon, Portugal) following the protocol described by [14].

To promote cyclic embryogenesis, the previously selected embryogenic line grown on ECO gelled medium was transferred to Erlenmeyer flasks containing 50 mL of liquid ECO medium with the same composition as the previous medium. To obtain sufficient material to further establish the experiment, the embryogenic cultures were maintained through three consecutive subcultures in fresh medium. Subcultures were performed every four weeks, with the cultures kept at 25 °C, in complete darkness, under 100 rpm orbital agitation.

To set up the experiment, approximately 200 mg of embryogenic *calli* was transferred into 100 mL Erlenmeyer flasks containing 50 mL of liquid ECO medium. Six Erlenmeyer flasks were prepared to further generate a pooled sample of CM (ECO culture medium collected four weeks after inoculation of embryogenic plant material). Simultaneously, six additional 100 mL Erlenmeyer flasks containing 50 mL of liquid ECO medium were prepared under the same conditions to serve as the control sample (ECO culture medium without inoculated embryogenic plant material).

2.2. Isolation of Secretome and Extracellular Metabolome from Conditioned Medium

The previously established Erlenmeyer flasks were left undisturbed for 5 min to allow the plant material to decant (procedure is represented in Figure 1). The CM was further collected from each Erlenmeyer flask in 50 mL tubes and centrifuged at 10,000× *g* for 10 min at 25 °C [51]. The collected supernatant was then filtered through a 0.45 µm filter and thereafter through a 0.22 µm filter using a vacuum system (Millipore, Burlington, MA, USA). The plant material settled at the bottom of the Erlenmeyer flasks was collected, flash-frozen with liquid nitrogen, and stored at −80 °C until further processing (see Section 2.3).

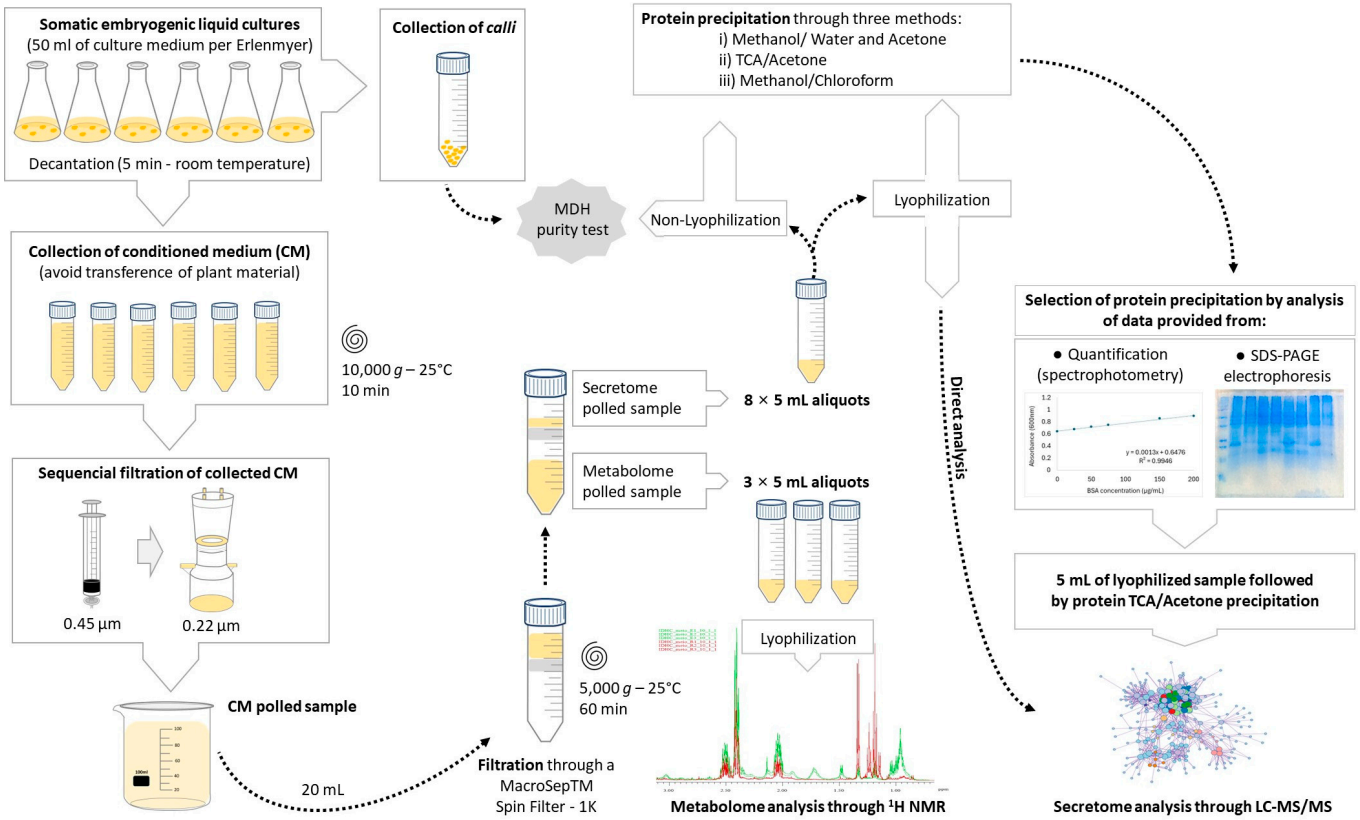

Figure 1. Workflow followed to collect and analyze the secretome and extracellular metabolome collected from liquid embryogenic cultures of *Olea europaea* L. Embryogenesis Cyclic Olive (ECO) culture medium was collected from replicates of an olive somatic embryogenic line that was initially selected and multiplied (see Section 2.1). This medium corresponds to the conditioned medium (CM). The collected CM was then filtered to separate the protein fraction from the metabolite fraction (for details, see Section 2.2). The purity of the protein extract was assessed by detecting MDH activity, using plant material collected from the same cultures as a positive control (see Section 2.3). For secretome precipitation, two approaches were tested, lyophilization and non-lyophilization, in combination with three different protein precipitation protocols. The efficiency of each method was evaluated through total protein quantification and SDS-PAGE electrophoresis (details in Section 2.4). For secretome analysis via LC-MS/MS, two approaches were tested (see Section 2.5): (i) sample obtained using the most efficient protein precipitation method (lyophilization of CM followed by total protein precipitation using the TCA/Acetone method); (ii) direct analysis of the lyophilized sample. For extracellular metabolome analysis, the fraction obtained from CM filtration was divided into 5 mL aliquots, lyophilized, and further analyzed through ^{1}H NMR (for details, see Section 2.6). For both secretome and extracellular metabolome analyses, a control sample was used, consisting of ECO medium with the same basal composition as CM but without the inoculation of plant material.

A pooled sample was prepared by combining the filtered samples collected from the six Erlenmeyer flasks. Proteins and metabolites were then separated using a MacroSep^{TM} Spin Filter 1K (PALL, New York, UK), which was pre-washed with 10 mL of RNase- and DNase-free sterile water, followed by centrifugation at 10,000× *g* for 10 min. The first step, the filtration step, was crucial for separating proteins from metabolites, retaining proteins (and some peptides larger than 1 kDa) above the filter while allowing metabolites to pass through. This process is particularly important for NMR analysis, as proteins, due to their large and complex structures, generate broad, overlapping signals in the NMR spectrum. These signals can obscure metabolite peaks, making accurate identification and quantification more challenging. Removing proteins not only enhances spectral clarity but also helps concentrate metabolites, improving detection sensitivity in NMR. Meanwhile,

the fraction containing the whole secretome was collected from the top of the 1K filter and divided into aliquots to test three different extraction methods, with and without sample lyophilization. However, it is important to note that the use of centrifugal filtration devices may introduce a potential sample loss step. Proteins may adsorb onto the filter membrane, reducing their recovery, or they may precipitate and aggregate due to increased local concentration during filtration. These factors should be carefully considered when interpreting results and optimizing protocols to minimize protein loss.

Due to the system's limitation (maximum volume of 20 mL), multiple centrifugation steps were performed at 5000× *g* for 60 min. The sample containing the whole secretome was collected from the top of the 1K filter, to which 1 mM phenylmethylsulfonyl fluoride (PMSF) was added to protect the sample from proteases. The total volume of the polled sample (~40 mL) was divided into 8 samples of 5 mL each to test the three different precipitation methods, with or without sample lyophilization. A 5 mL sample was lyophilized and directly used for LC-MS/MS analysis (see Section 2.5), and the remaining 5 mL sample was stored for further precipitation following the selected procedure and further analyzed through LC-MS/MS.

The sample containing the whole extracellular metabolome was collected from the bottom of the 1K filter. After sample collection (CM polled sample after all filtration procedure), three 5 mL aliquots were lyophilized and stored at −80 °C until further processing (see Section 2.6).

2.3. Analysis of the Secretome Purity Using a Cytosolic Biomarker

To confirm that the secretome did not contain contaminants from the cell interior, an assay using malate dehydrogenase (MDH), a cytosolic biomarker [52], was conducted comparing the collected secretome (see procedure in Section 2.2) with the total soluble proteins extracted from plant material (used as positive control). Embryogenic *calli* previous separated from the CM (Section 2.2) were ground with liquid nitrogen. A volume of 1.2 mL of extraction buffer [0.2 M Tris-HCL buffer (pH 8.2) solution containing 0.14 M NaCl, 0.05% (*v*/*v*) Tween-20, 0.2% (*w*/*v*) bovine serum albumin (BSA), 2% (*w*/*v*) Na_2SO_3, 2% (*w*/*v*) polyvinylpyrrolidone (PVP) K25, insoluble PVP (1:1, *w*/*w*)] was added to 150 mg of grounded embryogenic *calli*. Samples were vortexed and incubated on ice during 30 min with agitation. The homogenate was then centrifuged at 14,000× *g*, for 15 min at 4 °C [53], and the supernatant was collected. The protein content of the extracts was quantified based on the Bradford method using the Pierce™ 660 nm Protein Assay Reagent Kit (Thermo Scientific, Waltham, MA, USA).

An MDH analysis was performed using the sample extracted from plant material (positive control sample) and the collected secretome sample (see above 2.2). For that, 122.5 µL of each sample were mixed with 2% of IPG buffer (GE healthcare, Chicago, IL, USA) and applied by passive rehydration into immobilized nonlinear pH gradient 3-10 Immobiline Dry strips (7 cm) for 16 h at room temperature in the Multiphor II system (GE Healthcare). Each strip was covered with 2 mL of mineral oil (dry strip cover fluid) to prevent evaporation. Isoelectric focusing (IEF) was performed in Pharmacia LKB Multiphor II, at 12 °C, for 50 min at a constant voltage of 200 V, followed by another 50 min at a constant voltage of 400 V [54], followed by vertical separation NATIVE-PAGE gel in 14% acrylamide gels. In the NATIVE-PAGE separation, the strip containing the proteins previously separated by isoelectric focusing was placed on top of a resolving gel [14% polyacrylamide with 0.370 M Tris-HCl (pH 8.3), 14% acrylamide/bis-acrylamide, 0.07% ammonium persulfate (APS), and 0.05% tetramethyl ethylenediamine (TEMED)] and electrophoresis was carried out in a Mini-PROTEAN System (Bio-Rad, Hercules, CA, USA), filled with running buffer (25 mM Tris, 190 mM glycine) at a constant voltage of 130 V until the running front reaches

the end of the gel. Each sample was run in duplicate. NATIVE-PAGE gel was incubated, during 30 min, in 0.1 M Tris-HCL buffer pH 8.5 containing 0.025 (*w*/*v*) nicotinamide adenine dinucleotide (NAD), 10% (*v*/*v*) 1 M sodium hydrogen malate, 0.02% (*w*/*v*) nitroblue tetrazolium (NBT), 0.001% (*w*/*v*) phenazine methosulfate (PMS), in the dark at 40 °C [55]. The appearance/absence of protein spots was indicative of the presence/absence of the MDH enzyme.

2.4. Establishment of a Procedure for Secretome Precipitation and Characterization

2.4.1. Selection of the Most Efficient Method for Secretome Precipitation

To precipitate the secretome from the collected CM polled sample, three methods were tested: (i) Acetone precipitation [56], (ii) Trichloroacetic Acid (TCA)/Acetone precipitation [56], and (iii) Methanol/Chloroform precipitation [57]. The most efficient method for total protein precipitation was selected based on the quantification procedure through spectrophotometry, and on the protein band pattern evaluated through SDS-PAGE gel electrophoresis (described below in Section 2.4.3).

Acetone precipitation method: Amounts of 5 mL lyophilized and 5 mL non-lyophilized sample were mixed with a methanol/H_2O solution (80:20) (previously stored at −20 °C) in the 1:0.5 (*v*/*v*) and 1:4 (*v*/*v*) ratio, respectively. After vigorously mixing for 15 s, the samples were centrifuged (15,000× *g*, 4 °C for 10 min). The resulting pellets, with and without lyophilization, were mixed with 1 and 5 mL of ice-cold acetone, respectively, vigorously mixed for 15 s, and incubated overnight at −20 °C. The pellet (protein fraction) was collected by centrifugation under the conditions described above and washed with 1 and 5 mL of ice-cold acetone 90%, respectively, followed by centrifugation at 15,000× *g*, 4 °C, for 10 min. The purified pellets were air-dried for 1 h and then reconstituted in 1 mL of solubilization buffer (see Section 2.4.2).

TCA/Acetone precipitation method: Amounts of 5 mL lyophilized and 5 mL non-lyophilized sample were mixed with a methanol/H_2O solution (80:20) and centrifuged as described above. Subsequently, the resultant pellets from the culture medium, with and without lyophilization, were mixed with 1 and 5 mL of ice-cold acetone containing 20% TCA and 20 mM DTT, respectively, vigorously mixed for 15 s and incubated overnight at −20 °C. The pellet was collected by centrifugation under the conditions described above and washed with 1 and 5 mL of ice-cold acetone 90%, respectively, followed by centrifugation at 15,000× *g*, 4 °C, for 10 min. The purified pellets were air-dried for 1 h and then reconstituted in 1 mL of solubilization buffer (see Section 2.4.2).

Methanol/Chloroform precipitation: Amounts of 5 mL lyophilized and 5 mL non-lyophilized sample were mixed with ice-cold methanol in a 1:0.5 (*v*/*v*) and 1:4 (*v*/*v*) ratio, respectively, followed by vortexing for 15 s. Then, 5 mL of chloroform and 15 mL of Milli-Q sterile water were added to both samples, with vigorous mixing for 15 s between each reagent addition. Subsequently, the samples were centrifuged at 15000 ×g, room temperature, for 5 min. The pellet was collected and mixed with 20 mL of methanol. After gentle mixing, the samples were centrifuged at 15,000× *g*, 4 °C, for 10 min. The pellet was washed with 40 mL of ice-cold acetone 90%, followed by centrifugation at 15,000× *g*, 4 °C, for 10 min. The purified pellets were air-dried for 1 h and then reconstituted in 1 mL of solubilization buffer (see Section 2.4.2).

2.4.2. Protein Solubilization and Quantification

Following protein precipitation, the pellets were resuspended in 1 mL of solubilization buffer (7 M urea, 2 M thiourea, 4% CHAPS, 100 mM Tris-HCl, pH 7.5) and vortexed until fully solubilized. Total protein quantification was carried out using the Pierce™ 660 nm Protein Assay Reagent Kit (Thermo Scientific). To generate the calibration curve, bovine

serum albumin (BSA) concentrations of 125, 250, 500, 750, 1000, 1500, and 2000 µg/mL were used. In a 96-well microplate, 10 µL of each BSA solution or the same volume of each sample, in triplicate, was added to the wells. Subsequently, 150 µL of the Pierce™ 660 nm Protein Assay reagent was added to each well. Absorbance readings at 660 nm were taken using a Fluorescence multi-mode microplate reader GloMax® (Promega, Charbonnières-les-Bains, France). For each plate, a calibration curve was plotted based on the average absorbance values of each BSA standard against protein quantity. By interpolation and accounting for the dilution factor, the total protein concentration for each triplicate sample was calculated.

2.4.3. Analysis of the Secretome Band Patterns by SDS-PAGE

To evaluate the one-dimensional protein profile and determine the most effective protein precipitation method for the CM, the solubilized samples were subjected to SDS-PAGE following the method of Laemmli [58]. Each sample was tested in triplicate. The resolving gel (14% acrylamide) was prepared with 1.5M Tris-HCl pH 8.8, 0.1% of SDS, 14% acrylamide/bis-acrylamide, 5.45 mL of double-distilled water, 0.07% APS, and 0.05% TEMED. The stacking gel (4% acrylamide) was composed of 0.5M Tris-HCl pH 6.8, 0.1% SDS, 4% acrylamide/bis-acrylamide, 0.06% APS, and 0.11% TEMED. After polymerization, the gels were placed in the Protean Mini system (Bio-Rad) with running buffer (0.025 M Tris, 0.192M glycine, 1% (*w*/*v*) SDS). The samples were mixed with sample buffer (0.125 M Tris-HCl, pH 6.8, 1% (*w*/*v*) SDS, 5% 2-mercaptoethanol, 20% glycerol, trace amounts of bromophenol blue), heated to 37 °C for 10 min, and then cooled on ice before being loaded into the gel wells. A total of 35 µL of each sample was loaded per lane, and 4 µL of molecular weight marker (NZYA Colour Protein Marker II, Nzytech, Lisboa, Portugal) was added to each run. Electrophoresis was performed at a constant voltage of 130 V. At the end of the electrophoretic run, the gels were fixed for one hour in a solution of 40% methanol/10% acetic acid and stained for two hours with Coomassie Brilliant Blue (CBB) G-250 solution [59]. Gels were scanned in a scanning Molecular Dynamics densitometer with internal calibration using the LabScan 6.0 software (GE Healthcare). Images were analyzed using the GelAnalyzer software package (GelAnalyzer 2010a by Istvan Lazar, www.gelanalyzer.com).

2.5. Analysis of the Secretome by LC-MS/MS

After sample lyophilization and precipitation using the TCA/Acetone method, protein identification was carried out by LC-MS/MS analysis at the Proteomics Unit, National Centre for Biotechnology (Madrid, Spain). Protein cysteine residues were reduced and alkylated at 60 °C for 30 min with a buffer containing 5% SDS, 25 mM triethylammonium bicarbonate (TEAB), 5 mM tris(2-carboxyethyl) phosphine (TCEP), and 10 mM chloroacetamide (CAA). Protein digestion on S-Trap columns (Protifi, Huntington, NY, USA) was performed according to the previously established protocol [60]. Briefly, the precipitated sample was digested at 37 °C overnight using 1 µg of trypsin. Alternatively, the lyophilized sample (without precipitation) was directly loaded in the S-Trap columns. Tryptic peptides were cleaned up using home-made Stage-Tips prepared from Octadecyl C18 solid-phase extraction disks (Empore™, 66883-U, Stellarton, NS, Canada), as previously described [61]. Eluted peptides were dried in a speed vacuum and quantified by fluorimetry (QuBit) according to the manufacturer's instructions. Tryptic peptides were dried in a speed vacuum and quantified by fluorimetry (QuBit) according to the manufacturer's instructions.

For the analysis via nano-liquid chromatography coupled to electrospray ionization tandem mass spectrometry (nanoLC-ESI-MS/MS), 1 µg of each sample was individually analyzed using an Ultimate 3000 nano HPLC system (Thermo Fisher Scientific, Dreieich,

Germany) coupled online to an Orbitrap Exploris™ 240 mass spectrometer (Thermo Fisher Scientific, Germany). Each sample [1 µg in 5 µL of sample resuspended in mobile phase A: 0.1% formic acid (FA)] was loaded on a 50 cm × 75 µm Easy-spray PepMap C18 analytical column at 45 °C. Tryptic peptides were separated at a flow rate of 250 nL/min using a 90 min gradient ranging from 6% to 95% mobile phase B (80% acetonitrile (ACN) in 0.1% FA). To avoid carry-over, two 40 min blank samples (mobile phase A) were systematically run between samples. The instrument sensitivity was monitored through frequent injection of Pierce™ HeLa Protein Digest Standard (Thermo Scientific). Data acquisition was performed using a data-dependent top method, in full scan positive mode, scanning 375 to 1200 m/z. MS1 scans were acquired at an orbitrap resolution of 60,000 at m/z 200, with a normalized automatic gain control target of 300%, a radio frequency lens of 80%, and an automatic maximum injection time (IT). The top 20 most intense ions from each MS1 scan were isolated and fragmented with a higher-energy collisional dissociation (HCD) value of 30%. The resolution for HCD spectra was set to 15,000 at m/z 200, with a normalized AGC target of 50% and an automatic maximum IT. The precursor isolation window was 1.0 m/z, and dynamic exclusion (45 s) was applied. Precursor ions with single, unassigned, or six and higher charge states from fragmentation selection were excluded.

Raw data files were processed using the Proteome Discoverer 2.5.0.400 software (Thermo Scientific, Bremen, Germany), and database search was carried out using four search engines (Mascot (v2.8.0), MsAmanda (v2.4.0), MsFragger (v3.1.1), and Sequest HT against an *O. europaea* UniProtKB database (19 February 2021, 20,378 sequences) containing the most common laboratory contaminants (cRAP database with 69 sequences). Search parameters were set as follows: cysteine carbamidomethylation (+57.021464 Da); methionine oxidation (M) (+15.994915 Da), N-term acetylation (+42.010565 Da), and Gln→pyro-Glu (−17.026549 Da) as variable modifications. Precursor mass tolerances were set at 10 ppm and the fragment mass tolerance at 0.02 Da and trypsin/P was selected as a protease with a maximum of 2 missed cleavage sites. The false discovery rate (FDR) was calculated using the processing node Percolator (maximum delta Cn 0.05; decoy database search target) and an FDR ≤ 1% was considered for the validation of proteins and peptides. For protein identification, at least one unique peptide and a minimum of two peptide-spectrum matches (PSMs) were required. Protein abundance was also performed in Proteome Discoverer using the "Reporter Ions Quantifier" feature in the quantification workflow using the following parameters: unique+razor peptides; co-isolation threshold was set at 50%; signal to noise of reporter ions was 10; the normalization was performed considering the total peptide amount. The mass spectrometry proteomics data have been deposited to the ProteomeXchange Consortium via the PRIDE Archive—proteomics identification database [62] (https://www.ebi.ac.uk/pride/archive, accessed on 29 November 2024) with the dataset identifier PXD058411 and 10.6019/PXD058411.

A functional enrichment analysis of the identified proteins was visualized as a network of biological terms using Metascape (https://metascape.org) [63]. The enrichment analysis of proteins identified following the selected strategy was conducted using databases such as Gene Ontology (GO) [64] and the Kyoto Encyclopedia of Genes and Genomes (KEGG) [65] to identify statistically enriched terms. The resulting functional network integrated biological terms associated with the proteins set, where the size of the nodes are proportional to the number of proteins linked to each term was carried out using STRING (https://string-db.org/). Cytoscape 3.10.3 (https://cytoscape.org/) was used to map SE-related proteins across different biochemical pathways.

2.6. Analysis of the Extracellular Metabolome by 1H NMR Spectroscopy

The three lyophilized CM samples were further reconstituted in 1 mL of deuterated phosphate buffer (100 mM, pH 7.4) containing 0.1 mM trimethylsilylpropanoic acid (TSP-d4), and then centrifuged at 10,000× *g* for 10 min. The TSP-d_4 signal at 0 ppm was used for both chemical shift referencing and shimming, ensuring consistent spectral resolution and line width across all samples. A 550 µL portion of each supernatant was then transferred to a 5 mm NMR tube for analysis. The same procedure was followed using basal culture medium (ECO) not used for plant material subculture but maintained under the same conditions (control sample).

NMR spectra were recorded at the University of Aveiro on a Bruker Avance III HD 500 spectrometer, operating at 500.13 MHz for 1H observation. One-dimensional (1D) 1H spectra were collected at 298 K, with a total of 32 K data points, a spectral window of 7002.80 Hz, a relaxation delay of 2 s, and 512 scans, using the 'noesypr1d' pulse sequence. Data processing was conducted using TopSpin 4.0.3 (Bruker BioSpin, Rheinstetten, Germany), applying cosine multiplication (ssb 2), zero-filling to 64 k points, manual phasing, baseline correction, and calibration to the TSP-d4 reference signal at 0 ppm. Two-dimensional (2D) 1H-1H total correlation (TOCSY) spectra and J-resolved spectra were acquired for one sample to aid spectral assignment. For the semi-quantitative analysis of medium spectra, signal areas were measured using Amix-Viewer v. 3.9.15 (Bruker BioSpin, Billerica, MA, USA), and the variations were represented in a heatmap using Metaboanalyst 6.0. Since both ECO and cell-conditioned media (CM) were incubated under identical conditions, and all sample processing steps were carefully standardized; this approach allowed us to effectively determine metabolite consumption and secretion patterns.

3. Results and Discussion

3.1. Selection of the Most Efficient Method for Protein Precipitation

At the end of 21 days on induction OMc medium, radicles and cotyledons exhibited the development of *calli* (Figure A1a). At this point, all explants showing *callus* formation were transferred to OMc expression medium devoid of growth regulators to induce embryo differentiation. After 60 days, various *calli* exhibited somatic embryo development (Figure A1b), being further transferred to ECO culture medium to promote cyclic embryogenesis. Embryogenic lines that demonstrated a high number of somatic embryos were classified as highly competent embryogenic lines (Figure A1c). In contrast, low-competent embryogenic lines (Figure A1d) were characterized by a low number of developed embryos. The most competent embryogenic line, exhibiting a high number of somatic embryos, was selected and established in ECO liquid culture medium for subsequent secretome and extracellular metabolome analysis (conditioned medium—CM).

The CM, collected four weeks after the third subculture of the embryogenic line in ECO liquid medium, was first used to determine the most suitable protein precipitation method. Total protein quantification results across the three tested methods (Acetone, TCA/Acetone, and Methanol/Chloroform), with or without a prior sample lyophilization step, revealed a dependency on the precipitation method, with lyophilization being a crucial step (Table 1). The selection of the appropriate extraction method plays a crucial role in protein recovery, even when using highly sensitive techniques such as mass spectrometry. The correct approach to extraction and solubilization helps maximize protein recovery while minimizing interferences in subsequent steps, such as trypsin digestion. Although protein precipitation could introduce some protein loss, our results showed that the precipitation before LC-MS/MS analysis improved the protein recovery (see Section 3.2). Lyophilization, commonly referred to freeze-drying, is extensively employed across several sectors, including pharmaceuticals, cosmeceuticals, nutraceuticals, chemicals, and the food

industry [66]. This technique offers several advantages, such as concentrating the secretome [67], while not significantly affecting the stability of its proteins, lipids, and nucleic acids [68]. Abla et al. [69] also highlight the lyophilization procedure to preserve not only nucleic acids and proteins but also other sensitive materials, including microorganisms and nanoparticulate systems.

Table 1. Total protein concentration (µg/mL) across three precipitation methods tested lyophilized and non-lyophilized treatments.

Method	Lyophilized (µg/mL)	Non-Lyophilized (µg/mL)
Acetone	8.93	nt
TCA/Acetone	54.00	nt
Methanol/Chloroform	nt	nt

nt—not detected.

The TCA/Acetone method combined with sample lyophilization was the procedure that yielded the higher protein concentrations when compared with the other two methods (Table 1). SDS-PAGE gel electrophoresis confirmed those results, allowing the clear identification of six distinct bands (numbered 1 to 6, with apparent molecular weights ranging from 63 to 35 kDa) (Figure 2).

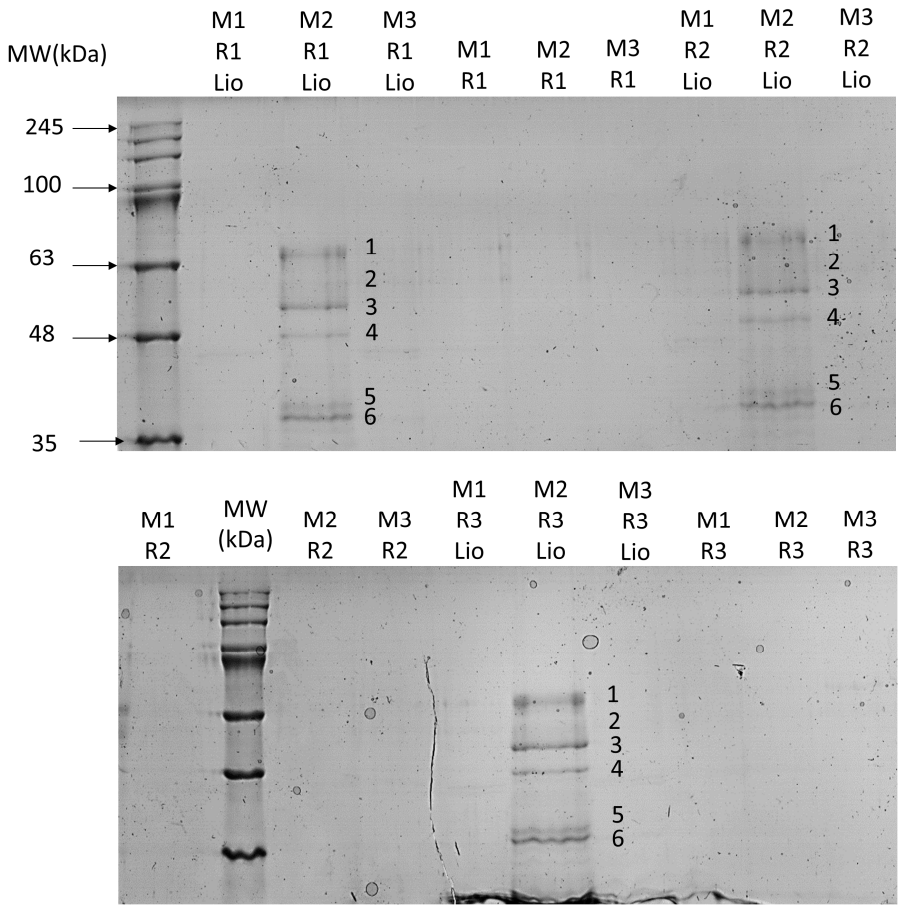

Figure 2. SDS-PAGE electrophoresis gel showing the band pattern achieved from analysis of samples precipitated with the three methods: Acetone precipitation method (M1), TCA/Acetone precipitation method (M2), and Methanol/Chloroform precipitation method (M3). Lyophilization procedure is identified by Lio. R1, R2, and R3 correspond to each technical replicate performed for each precipitation procedure. The six bands considered for the analysis of protein profiles are identified in the gel (numbered 1 to 6). MW—molecular weight marker (NZYA Colour Protein Marker II, Nztech) with the apparent size of each band indicated in kDa.

Of the six analyzed bands, the TCA/Acetone method was the only one present across all bands, showing higher protein concentration values compared to the other methods. However, significant differences were only observed in the lyophilized samples, specifically in band 5, corresponding to an apparent molecular mass of 30 kDa approximately, where the TCA/Acetone method outperformed the Acetone method. Notably, the band was not detected in samples processed with the Methanol/Chloroform method, which was expected considering the results achieved in the quantification procedure (results of statistical analysis presented in Table A1 of Appendix B).

The TCA/Acetone precipitation method relies on protein denaturation under acidic or hydrophobic conditions, which improve protein concentration and contaminant removal [70]. Compared to the two other tested methods, TCA/Acetone is well recognized for its ability to enhance protein yield, minimize degradation by protease activity, and reduce contamination from salts and polyphenols, factors that are critical for downstream applications [71,72]. By contrast, the Acetone precipitation method is limited by the requirement of a minimum 4:1 acetone-to-aqueous protein solution ratio, making it less practical for processing large sample volumes [73]. The Methanol/Chloroform precipitation method is specifically applied for recovering proteins from small, dilute samples, particularly those containing membrane proteins [57].

Based on the results, the TCA/Acetone precipitation method, combined with prior sample lyophilization, was the only protein precipitation method that successfully enabled protein precipitation thus allowing further analyses through high throughput platforms. The same method has proven highly effective for precipitating proteins, including low-molecular-weight proteins and extracellular proteins which often have low expression levels, in systems very similar to the liquid embryogenic cultures. There are examples of its application for concentrating extracellular enzymes released into the culture medium by *Pseudomonas* [74], and to isolate extracellular vesicles secreted by *P. aeruginosa* during biofilm development [75].

To assess the purity of the protein extract obtained through the selected procedure (TCA/Acetone precipitation after prior sample lyophilization), a protocol for the detection of cytosolic proteins was employed. The cytosolic biomarker MDH, an enzyme in the TCA cycle that catalyzes the reversible reduction of oxaloacetate to malate in the presence of NADH [52], was employed. This approach has been widely used to evaluate the purity of plant cellular fluids, such as extracted apoplastic fluids, in various plant species [76–78].

In the present research, the presence of the expected MDH spots in samples obtained from plant material (embryogenic *calli* collected from the CM) and their absence in the CM extract samples (Figure A2) confirmed the absence of cytosolic proteins in the CM sample. These results validate the effectiveness of the established workflow for isolating the secretome of liquid embryogenic cultures, enabling subsequent characterization studies.

3.2. LC-MS/MS-Based Analysis of Secretome from Embryogenic Calli

The strategy consisting of direct solubilization of 5 mL lyophilized sample without precipitation, followed by digestion with an S-trap column resulted in the identification and quantification of only 261 proteins/protein groups. This suggests that although this simpler strategy could help reduce protein losses, the presence of interfering substances may have affected trypsin digestion, leading to lower peptide recovery and a reduction in the number of identified proteins. In comparison, a total of 1111 proteins and 538 protein groups (FDR < 1%, PSM $\geq$ 2, at least a unique peptide), of which 1096 proteins (526 protein groups) correspond to *O. europaea* proteins (Table S1—Metascape results), were identified as part of the secretome of embryogenic *calli* using a strategy combining TCA/Acetone precipitation with prior sample lyophilization, protein digestion by S-trap and a proteomic

analysis by LC-MS/MS. Of these proteins, it was possible to measure the abundance of 994 *O. europaea* proteins (493 protein groups) in the sample, confirming that this strategy is the most appropriate for the analysis of the secretome of *O. europaea* cv. 'Galega Vulgar' embryogenic lines. Nevertheless, it should be taken into account that only a single replicate was analyzed using this final strategy. As a result, the outcomes might vary slightly with a higher number of replicates, particularly for the proteins identified with a single peptide.

The results obtained align with findings from similar proteomic analyses, although the number of identified proteins varies depending on the methodology used and the material analyzed. For instance, in tissue cultures, an LC-MS/MS-based proteomic analysis of *Elaeis guineensis* [79] identified approximately 4600 proteins and over 10,000 peptide sequences, significantly higher than the number identified in our study. In contrast, a recent study on the secretome of *P. nigra* [28] identified and quantified 187 proteins. Many of these proteins were products of complex gene families with multiple functions. While our study identified a substantially higher number of proteins, this broader identification likely reflects the complex nature of the secretome and the interactions occurring during somatic embryogenesis in *O. europaea*. Nevertheless, further analyses incorporating biological replicates will be necessary to ensure the reliability of the results and to accurately interpret protein expression patterns and their role in SE. An enrichment analysis allowed the identification of diverse canonical pathways with the identification of proteins with different biological functions, processes, and locations. Figure 3 represents different categories of protein ontology analysis. Each chart illustrates the percentage distribution of proteins associated with various biological categories, based on three primary aspects: biological component, biological function, and biological process. The results indicate a strong presence of proteins related to metabolism, catalytic activity, and intracellular processes, suggesting that the studied system is metabolically active and engaged in various cellular processes and responses to stimuli, including stress response as highlighted in previous reports [28,80–82].

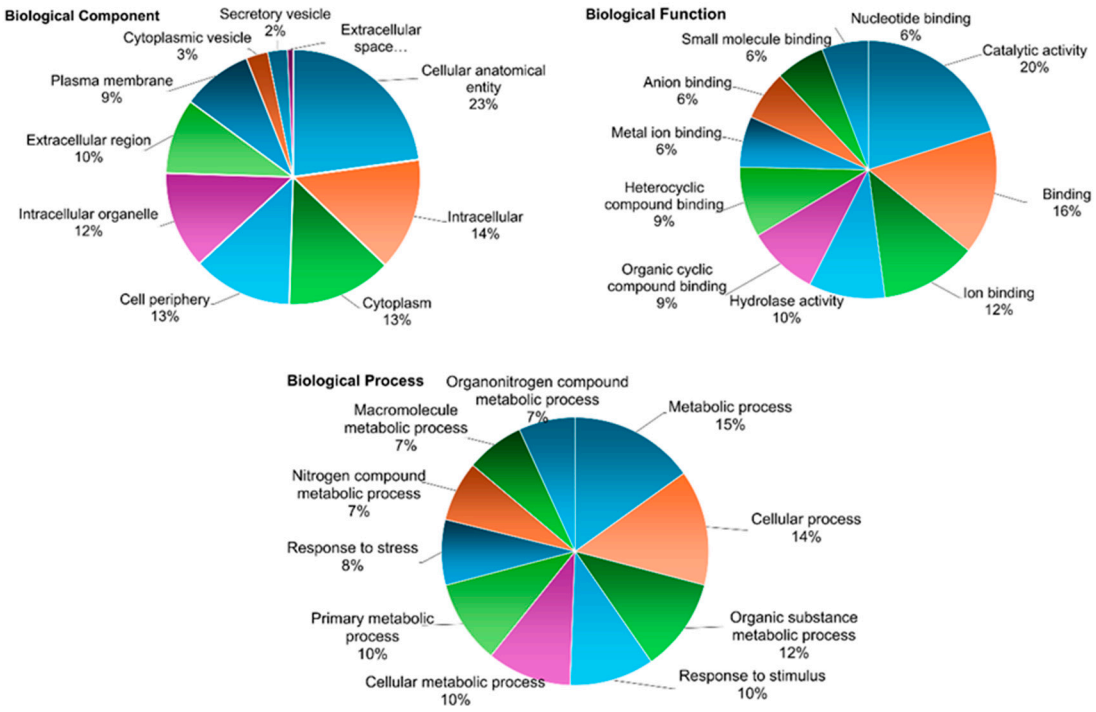

Figure 3. Distribution of proteins identified in the secretome of olive (*Olea europaea* subsp. *europaea* L.) somatic embryogenic liquid cultures. The circular charts illustrate the relative proportions of putative biological components, key functions, and associated processes of the proteins, highlighting their roles within the precipitated secretome.

In analyzing the biological component, the presence of proteins originating from intracellular organelles and the cytoplasm in the extracellular space can be attributed to exocytosis processes. Exocytosis is an energy-consuming process that expels secretory vesicles containing nanoparticles out of the cell membranes and into the extracellular space [83]. These membrane-bound vesicles contain soluble proteins, membrane proteins, and lipids, and subsequently fuse with the cell membrane for secretion into the extracellular environment [84]. Lysosomes, which contain a range of hydrolytic enzymes for degrading cellular materials, also play a crucial role in exocytosis [85]. Specifically, these organelles can extracellularly release their contents via lysosomal exocytosis, involving the fusion of lysosomes with the plasma membrane to discharge their enzymes and other substrates into the extracellular space [86]. Furthermore, exocytosis can be induced by changes in environmental conditions or by cellular stress signals, reflecting the cell's ability to adapt and modulate its interactions with the microenvironment [87]. Thus, the detection of intracellular organelles and the cytosolic proteins in the CM may indicate an active cellular state, where communication and interaction with the external environment are essential to its functionality. The role of cytosolic proteins in regulating cellular processes related to organelle function and environmental interactions has been reported in various studies. For example, HSP type 2 was found to be upregulated during SE induction in *Cyathea delgadii* [81], while cytosolic HSP18.2 and class II HSP17.6 were upregulated during somatic embryo development in *P. pinaster* [88].

Regarding biological putative functions, a total of 78 were identified. The most prevalent processes identified are related to metabolic functions, specifically cellular metabolism and the metabolism of organic substances. These metabolic processes play a crucial role during SE, as cells transition from a somatic to an embryogenic state. During this transition, cells undergo dedifferentiation, activate their cell division cycle, and reorganize their metabolic and physiological states [89]. Among these processes, metal ions are vital, serving to bridge distant residues or domains within proteins, mediating interactions between proteins and ligands, and functioning within the active site as nucleophilic catalysts and electron transfer agents [90]. In proteins, metal ions are crucial for maintaining structural integrity, regulatory functions, and enzymatic activity, all of which are essential for sustaining homeostasis and supporting complex cellular networks [91]. The binding of specific metal ions can stabilize proteins or protein domains [92]. Among the identified proteins, ascorbate peroxidase 1 (APX1) has been reported to play a significant role in SE, being involved in tissue protection. A study examining embryogenic and non-embryogenic *calli* from *Medicago arborea* [93] investigated POX activity. The results showed a decrease in soluble POX activity in the embryogenic *calli* at the time when somatic embryos began to emerge. According to several authors, SE is a plant cell response upon abiotic stresses [94], and the initiation and differentiation of SE is regulated by the redox balance within embryogenic tissues, and an increase in oxidative stress levels is necessary to promote the formation of embryogenic cells [95,96].

The enrichment analysis identified statistically significant terms, including GO terms and KEGG pathways, based on cumulative hypergeometric *p*-values and enrichment factors (Figure A3). These terms were hierarchically organized into clusters using Kappa statistical similarity, with a threshold of 0.3, grouping terms that share common proteins. The most significant cluster includes terms related to the recognition of pollen, other glycan degradation, phenylpropanoid biosynthesis, and external encapsulating structure organization, suggesting that the identified proteins play a central role in SE. The results suggest that the most enriched processes involve pollen recognition and the metabolism of carbohydrates and phenolic compounds (Figure A4). Pollen recognition is likely associated with mechanisms of self-incompatibility or selective fertilization. Among the identified

proteins, RK3 stands out as a member of the plant receptor-like kinase (RLK) family. These proteins are composed of an extracellular domain, a single transmembrane segment, and an intracellular kinase domain. The extracellular region of RLKs is highly diverse, featuring specialized domains that enable ligand recognition and signal perception. This structural variability allows RLKs to function as key cell surface receptors, mediating crucial biological processes such as development and stress responses in SE [97].

The functional enrichment analysis of the identified proteins was visualized as a network of biological terms using Metascape (Figure 4). The most significant terms include glycan degradation and phenylpropanoid biosynthesis. This aligns with findings from a study on *P. koraiensis* [80], where different SE cell lines were analyzed, revealing significant enrichment in phenylpropanoid biosynthesis, starch and sucrose metabolism, and glycan degradation pathways in responsive SE cells compared to blocked or non-SE cell lines. Additionally, the organization of external encapsulating structures relates to the organization of the cell wall or extracellular structures [98]. Starch and sucrose metabolism are indicated as a key metabolic process involved in SE. In fact, carbohydrates can act as signaling molecules and regulators of gene expression, as part of signaling networks connecting the environment with plant metabolism, development, and growth [99]. Among the identified proteins, α-amylase (AMY, including AMY1 and AMY2), a hydrolase that catalyzes the breakdown of internal α-(1–4)-glycosidic bonds in starch, glycogen, and related oligosaccharides, play a key role in energy and carbon metabolism by processing environmental polysaccharides [100]. AMYs are typically secretory proteins that are biosynthesized in the secretory tissues, such as the scutella epithelium and the aleurone layer, before being secreted into the starchy endosperm [101]. In a recent study using SE suspension cell cultures of *P. nigra*, Pernis et al. [28] identified the AMY protein secreted into the culture medium. The authors found that this protein was more abundant in the medium of lines with high embryogenic capacity. The detection of this enzyme in the secretome in this study may indicate an important role in SE and its potential as a molecular marker.

The generated network reveals various interrelated clusters of biological terms, reflecting the biological processes associated with the set of proteins identified in the secretome of the embryogenic line. Terms with a higher number of associated proteins indicate groups that share proteins or have related biological functions, suggesting that these processes are highly relevant within the context of SE. The interactions among these terms highlight potentially interconnected biological pathways. Smaller clusters can also be observed in Figure 4, such as the group of terms associated with the hydrogen peroxide (H_2O_2) catabolic process, represented by proteins like mitochondrial Peroxiredoxin-IIF (PRXIIF) and thioredoxin peroxidase (TPX1). These proteins are linked to pathways related to antioxidant activity, catalytic activity, and POX activity. H_2O_2 is a significant REDOX molecule that, at high concentrations, induces oxidative damage to biomolecules. In a study on SE in olive, Oulbi and co-workers [82] observed higher POX activity in embryogenic cultures compared to non-embryogenic cultures for the zygotic explants of cv. 'Picholine Marocaine' and cv. 'Dahbia'. Their results suggest that POX enzymes may be involved in secondary or adaptive mechanisms during SE and could potentially serve as biochemical markers. Ultimately, the results highlight the important role of secreted proteins in SE, particularly the involvement of plant α-amylases in carbohydrate metabolism and H_2O_2 in catabolic processes and signaling pathways. A better understanding of these secreted proteins improves our knowledge of the metabolic adaptations that support SE and the viability of plant cells in culture.

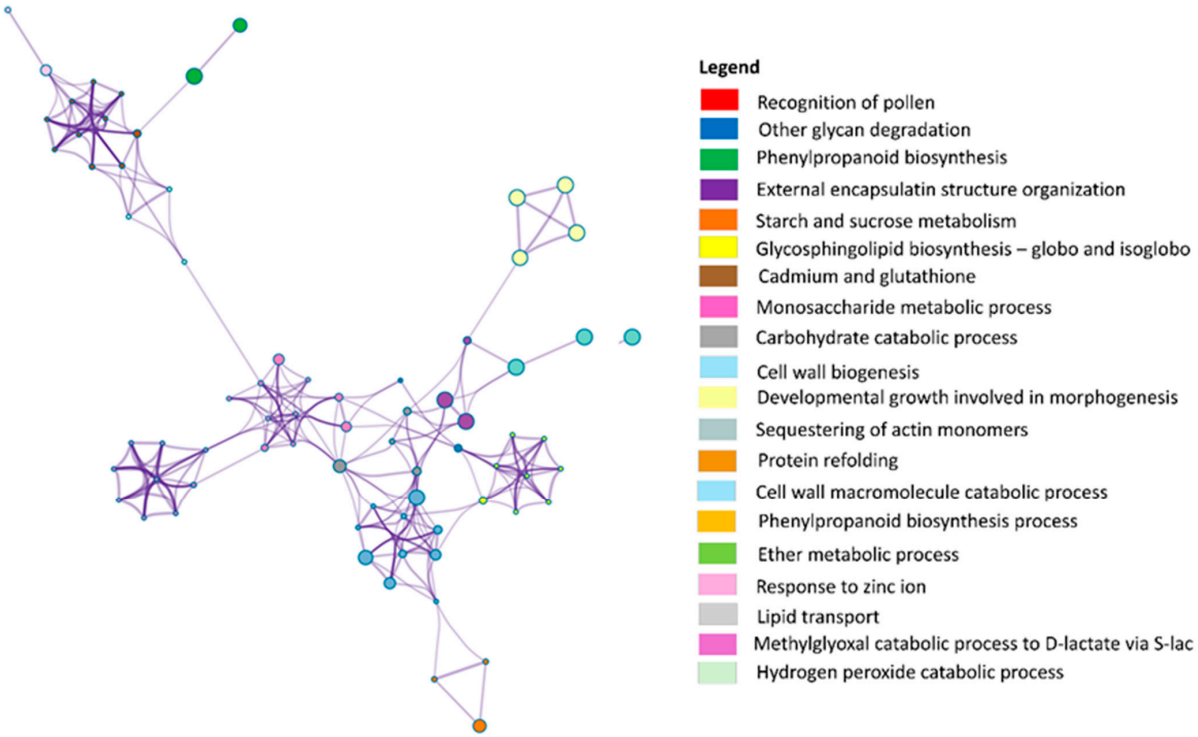

Figure 4. Network of identified biological terms constructed using Metascape (https://metascape.org), where each circle represents a term, and the size of the circle indicates the number of associated proteins. The colors represent clusters of related terms. The connections (edges) between nodes reflect functional similarity, with the thickness of the connections indicating the degree of similarity (score > 0.3). Larger nodes represent terms that are widely represented by the identified proteins, suggesting significant relevance of these processes in the proteomic analysis. Thicker connections between terms indicate high similarity, highlighting interrelated biological processes.

3.3. Detection of Changes in the Exametabolome Composition Through 1H NMR Spectroscopy

NMR spectroscopy enabled the identification of various components in both the ECO basal medium (negative control) and the CM collected for growing embryogenic *calli*. In total, 20 metabolites were unambiguously identified, including amino acids, sugars, organic acids, and alcohols. Figure 5A shows representative spectra retrieved from both samples. Several amino acids were identified in the ECO medium, likely originating from the casein hydrolysate used in its preparation. The hydrolyzed form of casein plays a crucial role in SE by providing essential nutrients that support cellular growth and development. Casein is a phosphoprotein that comprises four distinct subunits (αs1-, αs2-, β-, and κ-casein) varying in their primary structure and the type and extent of post-translational modifications [102]. Casein hydrolysates are a rich source of calcium, phosphate, various microelements, vitamins, and, most importantly, a mixture of up to 18 amino acids [89].

The results indicate that embryogenic cells consumed significant amounts of several amino acids, including methionine (−75.5 ± 13.4% vs. ECO medium), tryptophan (−74.4 ± 12.2%), lysine (−76.2 ± 12.1%), phenylalanine (−88.7 ± 13.1%), tyrosine (−92.8 ± 12.7%), branched chain amino acids—valine, leucine, and isoleucine (−88.4 ± 14.0%)—and alanine (−84.9 ± 11.6%) (Figure 5B). The aromatic amino acids tyrosine and phenylalanine are known to serve as crucial substrates for producing secondary metabolites that plants use to counteract stress [103]. Additionally, embryogenic cells consumed 58.6 ± the pyroglutamate (formed through the non-enzymatic cyclization of glutamine) present in the ECO medium. Amino acids in the glutamine/glutamate family play key roles in initiating and accelerating the incorporation of ammonia and nitrite into organic nitrogen metabolism [104]. These amino acids function as nitrogen storage com-

pounds [105], act as intermediates for incorporating ammonia into amino acids, and serve as building blocks for proteins or nucleotides [106]. Thus, these amino acids are an efficient nitrogen source for direct protein synthesis [107] and facilitate nitrogen assimilation during long-distance metabolic transport [108]. A recent study identified amino acids as key regulators of morphogenesis during SE in *Litchi chinensis* Sonn. cv. 'Feizixiao' [109], demonstrating their positive influence on *callus* proliferation and embryo induction. When supplied in specific mixtures, amino acids significantly enhanced somatic embryo regeneration. These findings highlight their role not only as an efficient nitrogen source for protein synthesis and metabolic transport but also as crucial factors in optimizing in vitro regeneration protocols, supporting our observations of their contribution to nitrogen assimilation during SE.

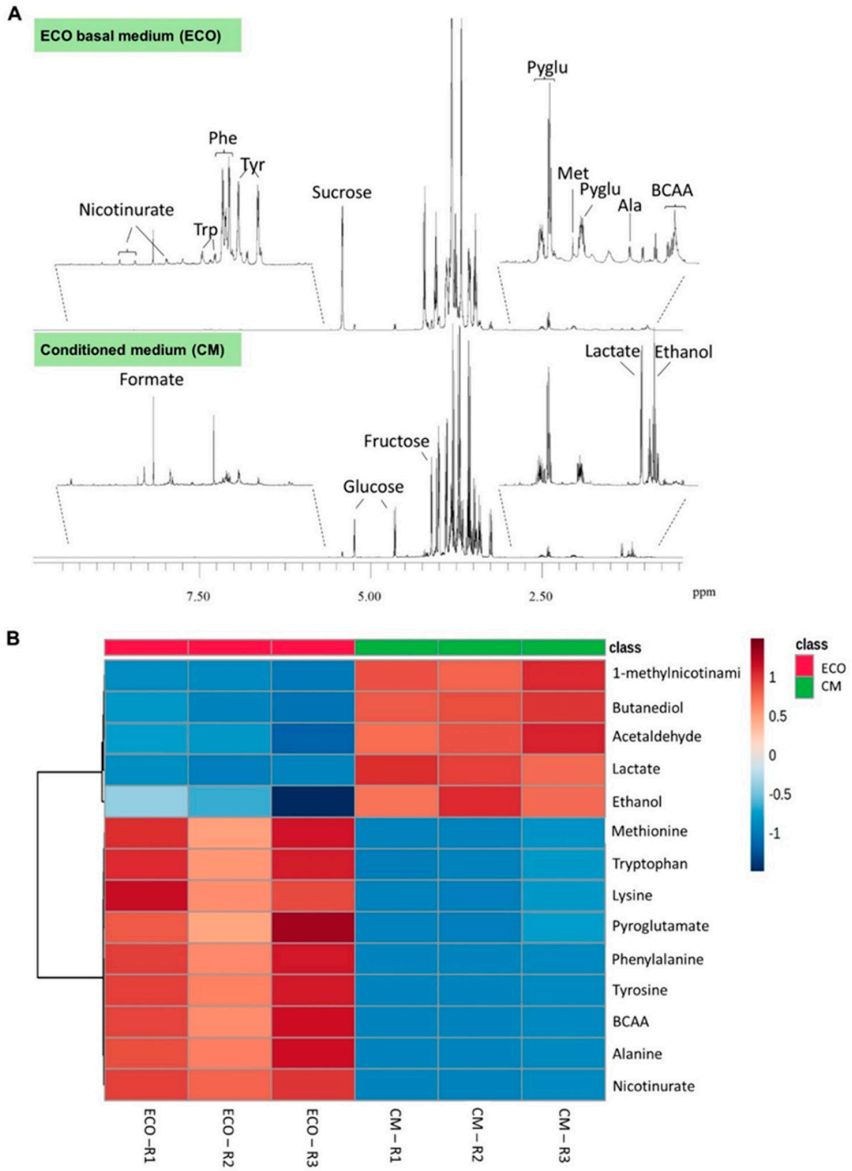

Figure 5. NMR analysis of conditioned medium (CM) samples (ECO medium collected four weeks after inoculation of embryogenic pant material), and ECO samples (ECO medium not inoculated with embryogenic plant material but maintained under the same photoperiod and temperature conditions as that those of the CM samples). (**A**) Representative 1H NMR spectra with key signals assigned to major metabolites. (**B**) Heatmap displaying the relative abundance of metabolites with statistically significant differences between the two sample types. R1, R2, and R3 correspond to the three replicates considered for each type of sample.

Regarding the metabolites secreted into the medium by embryogenic cells, they included 1-methylnicotinamide (MNA), 2,3-butanediol, acetaldehyde, lactate, and ethanol (Figure 5B). The secretion of MNA suggests that the cells may be methylating nicotinamide as part of a detoxification or regulatory process to maintain NAD+ homeostasis. The consumption of nicotinurate (conjugate of nicotinic acid and glycine, both used in the preparation of the ECO medium) is consistent with the active regulation of NAD+ metabolism.

The secretion of 2,3-butanediol, acetaldehyde, lactate, and ethanol suggests a metabolic shift that could involve anaerobic or microaerobic processes. These metabolites are typically associated with fermentation pathways, which may serve to regenerate NAD^+ and sustain glycolytic flux under specific metabolic conditions. For instance, the production of 2,3-butanediol involves the conversion of pyruvate to acetoin, followed by its reduction to 2,3-butanediol. This pathway helps regenerate NAD^+ from NADH, allowing glycolysis to continue. Similarly, acetaldehyde is a key intermediate in ethanol fermentation, where pyruvate is decarboxylated to form acetaldehyde, which is then reduced to ethanol by alcohol dehydrogenase. Lactate production, typically arising from lactic acid fermentation, results from the reduction of pyruvate in the absence of sufficient oxygen, again facilitating NAD^+ regeneration. While these metabolic shifts are often linked to low oxygen availability, we acknowledge that our study does not directly measure dissolved oxygen levels in the culture medium. Thus, although our results are consistent with metabolic adaptations observed under hypoxic conditions, we cannot conclusively attribute them to oxygen limitation. Additionally, alternative biochemical pathways could contribute to the detected metabolites, and the presence of fermentation intermediates does not necessarily confirm a predominant reliance on anaerobic metabolism.

Moreover, some of these metabolites could result from extracellular enzymatic activity rather than direct cellular secretion. If cells release enzymes capable of metabolizing medium components, these transformations could influence the observed metabolite profile. Passive diffusion of small molecules between cells and the extracellular environment may also contribute. However, the coordinated presence of these metabolites, particularly intermediates of known fermentation pathways, suggests that they primarily originate from active cellular metabolism rather than random extracellular reactions. Future studies incorporating direct oxygen measurements, as well as gene expression or enzymatic analyses, will be necessary to further elucidate the metabolic state of these cells.

In the context of SE, sucrose in the basal medium is essential for the maintenance and maturation of somatic embryos, serving as a primary source of metabolic energy and carbon during embryo development [1,108]. These compounds act as osmotic agents, helping to preserve the integrity of the plasma membrane [110], and may also function as reserve compounds or contribute to desiccation stress tolerance during SE process [111]. An analysis of 1H NMR spectra showed that sucrose was hydrolyzed into glucose and fructose, which were clearly detected in the CM spectra (Figure A4). In fact, plant α-amylases are enzymes that contribute to the hydrolysis of starches, while sucrose itself is hydrolyzed into glucose and fructose by specific enzymes, such as invertase [112]. Consequently, the production of glucose and fructose from sucrose may be influenced by the activity of amylases, which can enhance the efficiency of this hydrolysis, particularly under stress conditions or during cellular development. Interestingly, the total amount of glucose and fructose detected was similar to the initial amount of sucrose, suggesting that there was minimal consumption of these sugars by the cells (Figure A4). This observation likely raises a question about the key biological roles played by and the production of metabolites such as 2,3-butanediol, acetaldehyde, lactate, and ethanol, which are typically derived from the breakdown of glucose through glycolysis and subsequent fermentation. One possible explanation for this apparent discrepancy is that the cells may be utilizing an alternative

metabolic pathway or external source of carbon to produce these metabolites. For instance, the cells might be relying on internal reserves, such as starch or other polysaccharides that are not directly reflected by the sugars measured in the medium. Another possibility is that the observed production of fermentation by-products could result from alternative pathways involving other carbon sources or the regeneration of NAD+ through anaerobic or microaerobic conditions, independently of the sugar consumption.

Overall, our results highlight the complex metabolic processes occurring in embryogenic plant cells, including the active regulation of NAD+ homeostasis, the utilization of amino acids and alternative carbon sources, and the engagement of fermentation pathways under oxygen-limited conditions. These findings contribute to a better understanding of the metabolic adaptations that support SE and the survival of plant cells in culture.

4. Conclusions

The present study outlines an efficient protocol for separating proteins and metabolites secreted by olive (*O. europaea* subsp. *europaea* L.) embryogenic cultures during cyclic embryogenesis in ECO liquid culture medium. The application of LC-MS/MS and NMR techniques proved highly effective for identifying and relatively quantifying these secreted biomolecules, underscoring their potential for a detailed analysis of cellular secretions. The results reveal that numerous proteins and metabolites are secreted into the extracellular environment, accumulating as they are released by explants during the SE process. The findings of this study lay the groundwork for a deeper understanding of the molecular mechanisms governing SE. By establishing an efficient workflow, this research enables future comparisons between high- and low-efficiency embryogenic lines to identify key molecules that regulate and enhance SE in olive.

Supplementary Materials: The following supporting information can be downloaded at: https://www.mdpi.com/article/10.3390/horticulturae11030331/s1, Table S1: Metascape result.

Author Contributions: Conceptualization R.P., F.M.S., A.P., and H.C.; methodology, R.P., L.R., F.M.S., S.C., I.F.D., and H.C.; formal analysis, R.P., L.R., F.M.S., I.F.D., and H.C.; investigation, R.P., L.R., F.M.S., I.F.D., S.C., A.P., and H.C.; supervision, H.C. and A.P.; writing—original draft preparation, R.P., L.R., F.M.S., I.F.D., and H.C.; writing—review and editing, R.P., L.R., F.M.S., I.F.D., S.C., A.P., and H.C. All authors have read and agreed to the published version of the manuscript.

Funding: This work is funded by National Funds through FCT—Foundation for Science and Technology under the Project UIDB/05183. This work was also developed within the scope of the projects CICECO-Aveiro Institute of Materials (UIDB/50011/2020, DOI 10.54499/UIDB/50011/2020; UIDP/50011/2020, DOI 10.54499/UIDP/50011/2020; LA/P/0006/2020, DOI 10.54499/LA/P/0006/2020), and LAQV-REQUIMTE (LA/P/0008/202, DOI 10.54499/LA/P/0008/2020; UIDP/50006/2020, DOI 10.54499/UIDP/50006/2020; UIDB/50006/2020, DOI 10.54499/UIDB/50006/2020), financed by national funds through the FCT/MCTES (PIDDAC). The NMR spectrometer is part of the National NMR Network (PTNMR) and is partially supported by Infrastructure Project Nº 022161.

Data Availability Statement: The original contributions presented in the study are included in the article/supplementary material, further inquiries can be directed to the corresponding author.

Acknowledgments: The authors would like to thank to MED for the support given through the exploratory project ID 10_2021 ("Unravelling olive somatic embryogenesis signalling—a focus on the extracellular bioactive molecules"). R.P. would like to thank FCT for the support provided through the funding of the PhD fellowship with reference UI/BD/153509/2022. F.M.S acknowledges their contract Sara Borrel "CD23/00049" funded by grants from the Instituto de Salud Carlos III (ISCIII).

Conflicts of Interest: The authors declare no conflicts of interest.

Abbreviations

The following abbreviations are used in this manuscript:

SE	Somatic embryogenesis
CM	Conditioned medium
SDS-PAGE	Sodium dodecyl sulfate–polyacrylamide gel electrophoresis
LC-MS/MS	Liquid chromatography coupled to mass spectrometry
NMR	Nuclear Magnetic Resonance
OMc	Olive Medium Culture
ECO	Embryogenesis Cyclic Olive
MDH	Malate dehydrogenase
NAD	Nicotinamide adenine dinucleotide
TCA	Trichloroacetic acid
AMY	α-amylase
POX	Peroxidase

Appendix A

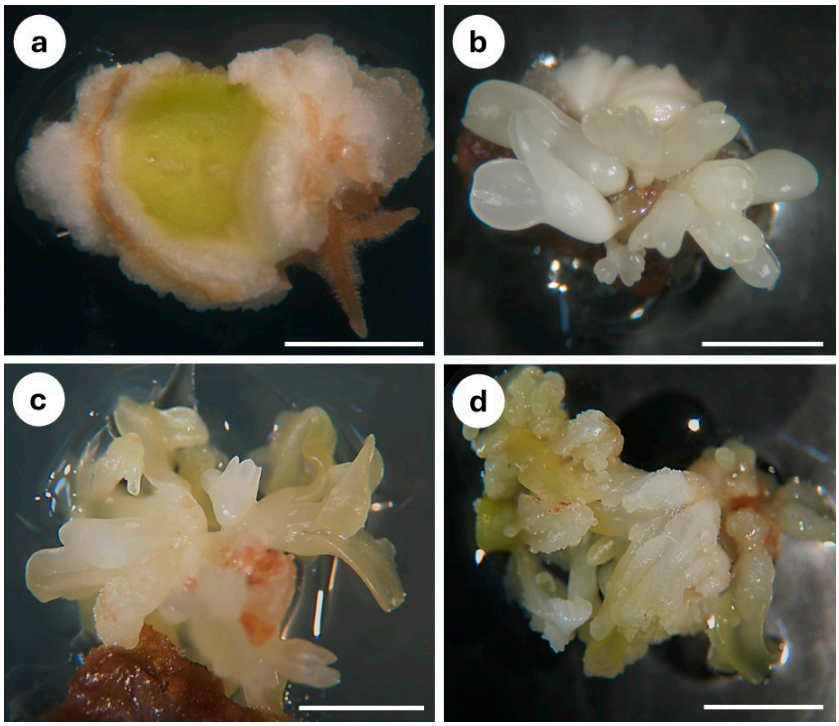

Figure A1. Explants from cv. 'Galega Vulgar' at the end of the induction phase (**a**) and expression phase (**b**). High embryogenic efficient line (**c**) and low embryogenic efficient line (**d**) in cyclic embryogenesis in liquid ECO culture medium. Bars: 0.5 cm.

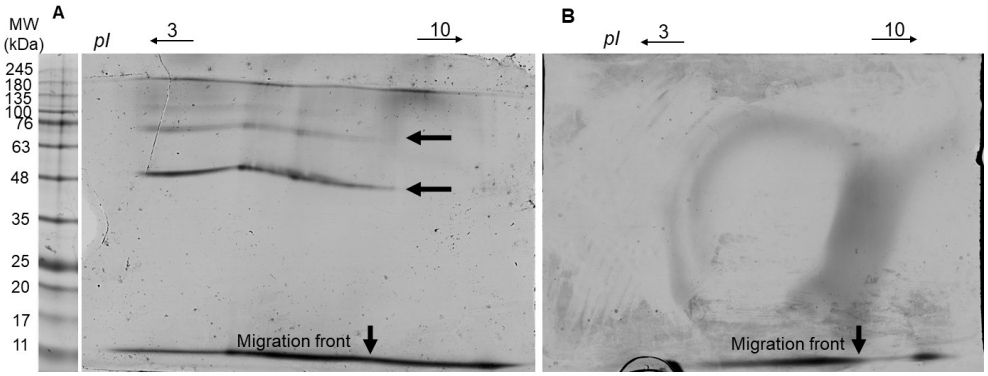

Figure A2. Identification of MDH isoenzyme activity following isoelectric focusing on polyacrylamide gels stained with malate, NAD+, and nitroblue tetrazolium. The appearance of protein spots in sample obtained from plant material indicates the presence of the MDH enzyme (black arrows) (**A**); the absence of those spots in CM reveals no presence of MDH enzyme and consequently no contamination by proteins in precipitated secretome from the CM (**B**). MW—molecular weight marker (NZYA Colour Protein Marker II, Nztech) with the apparent size of each band indicated in kDa; pI—isoelectric point.

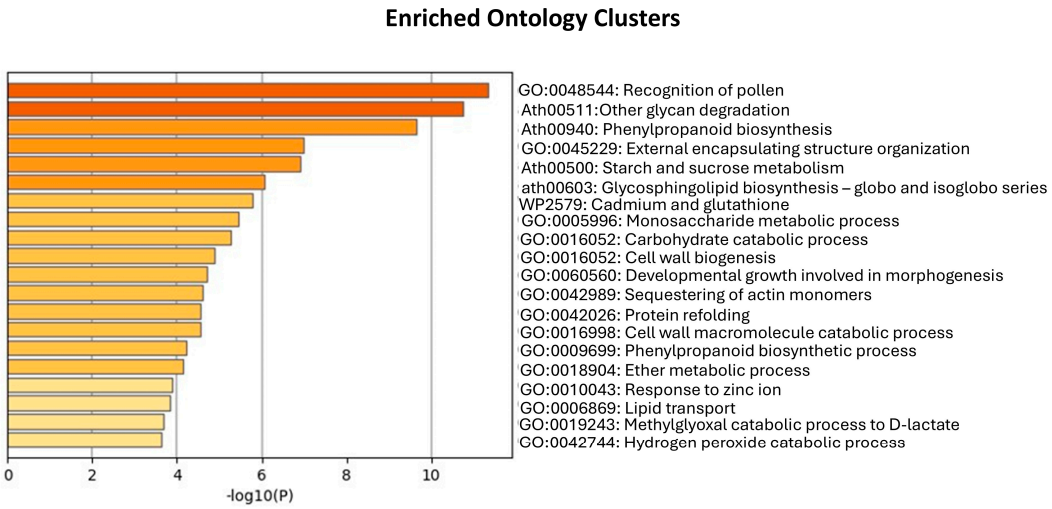

Figure A3. Enriched ontology clusters corresponding to biological processes. Statistical significance of the enrichment is indicated by −log10 (*p*-value).

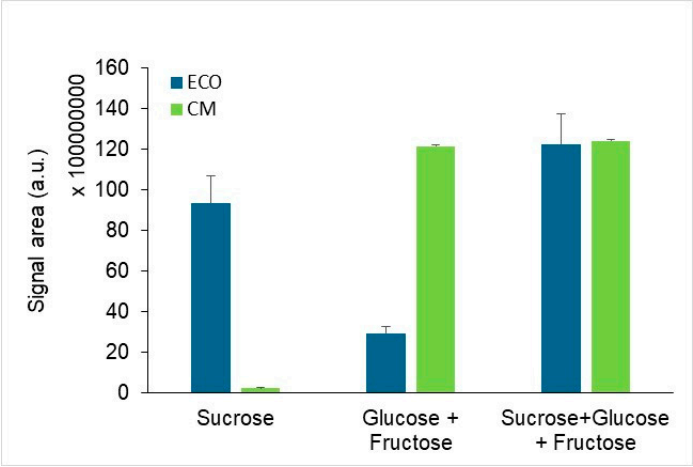

Figure A4. Quantification of sucrose, glucose, and fructose levels in ECO (control sample established without plant material) and CM samples using NMR spectroscopy. The signal area (a.u.) for each

sugar component, as well as their combinations, is displayed, highlighting differences between ECO (dark blue) and CM (light green) samples. Error bars represent the standard deviation of measurements.

Appendix B

Table A1. Expression level of protein bands (numbered 1 to 6) considered for the comparative analysis of precipitation methods. Significant differences in expression band levels among the three protein precipitation methods (Acetone, TCA/Acetone, and Methanol/Chloroform) are indicated by different letters, which denote statistically significant differences ($p \leq 0.05$).

Precipitation Methods				
Lyophilized				
Bands	**Acetone**	**TCA/Acetone**	**Methanol/Chloroform**	***p*-Value**
1	291.3 ± 291.3	1849.7 ± 464.5	381.7 ± 381.7	0.052
2	324.7 ± 324.7	1807.7 ± 158.4	378.3 ± 378.3	0.052
3	326.3 ± 326.3	1762.7 ± 33.7	319.3 ± 319.3	0.052
4	409.3 ± 409.3	851.7 ± 429.7	262.0 ± 262.0	0.5
5	456.4 ± 456.3 a	1598.0 ± 94.92 b	nt	0.035
6	381.0 ± 381.0	607.3 ± 607.33	525.3 ± 262.7	0.948
Non-lyophilized				
1	146.0 ± 146.0	877.3 ± 114.9	547.7 ± 279.2	0.120
2	399.7 ± 201.6	506.0 ± 253.8	291.3 ± 291.3	0.794
3	nt	612.3 ± 313.5	337.0 ± 337.0	0.281
4	184.3 ± 184.3	366.7 ± 366.7	nt	0.558
5	491.0 ± 249.5	522.7 ± 271.3	294.0 ± 294.0	0.854
6	nt	443.0 ± 443.0	nt	0.368

nt—not detected.

References

1. Juarez-Escobar, J.; Bojórquez-Velázquez, E.; Elizalde-Contreras, J.M.; Guerrero-Analco, J.A.; Loyola-Vargas, V.M.; Mata-Rosas, M.; Ruiz-May, E. Current Proteomic and Metabolomic Knowledge of Zygotic and Somatic Embryogenesis in Plants. *Int. J. Mol. Sci.* **2021**, *22*, 11807. [CrossRef] [PubMed]
2. Hazubska-Przybył, T.; Ratajczak, E.; Obarska, A.; Pers-Kamczyc, E. Different Roles of Auxins in Somatic Embryogenesis Efficiency in Two *Picea* Species. *Int. J. Mol. Sci.* **2020**, *21*, 3394. [CrossRef] [PubMed]
3. Vidal, N.; Mallón, R.; Valladares, S.; Meijomín, A.M.; Vieitez, A.M. Regeneration of Transgenic Plants by Agrobacterium-Mediated Transformation of Somatic Embryos of Juvenile and Mature *Quercus robur*. *Plant Cell Rep.* **2010**, *29*, 1411–1422. [CrossRef] [PubMed]
4. Heringer, A.S.; Santa-Catarina, C.; Silveira, V. Insights from Proteomic Studies into Plant Somatic Embryogenesis. *Proteomics* **2018**, *18*, 1700265. [CrossRef]
5. Guan, Y.; Li, S.-G.; Fan, X.-F.; Su, Z.-H. Application of Somatic Embryogenesis in Woody Plants. *Front. Plant Sci.* **2016**, *7*, 938. [CrossRef]
6. Pais, M.S. Somatic Embryogenesis Induction in Woody Species: The Future After OMICs Data Assessment. *Front. Plant Sci.* **2019**, *10*, 240. [CrossRef]
7. Trabelsi, E.B.; Bouzid, S.; Bouzid, M.; Elloumi, N.; Belfeleh, Z.; Benabdallah, A.; Ghezel, R. In-Vitro Regeneration of Olive Tree by Somatic Embryogenesis. *J. Plant Biol.* **2003**, *46*, 173–180. [CrossRef]
8. Brhadda, N.; Abousalim, A. Loudyi Dou Elmacane Walali Effets du milieu de culture et de la lumière sur l'embryogenèse somatique de l'olivier (*Olea europaea* L.) cv. Picholine marocaine. *Fruits* **2003**, *58*, 167–174. [CrossRef]
9. Capelo, A.M.; Silva, S.; Brito, G.; Santos, C. Somatic Embryogenesis Induction in Leaves and Petioles of a Mature Wild Olive. *Plant Cell Tiss. Organ Cult.* **2010**, *103*, 237–242. [CrossRef]
10. Oulbi, S.; Belkoura, I.; Loutfi, K. Somatic Embryogenesis from Somatic Explants of a Moroccan Olive (*Olea europaea* L.) Cultivar, 'Moroccan Picholine'. *Acta Hortic.* **2018**, *1199*, 91–96. [CrossRef]

11. Mazri, M.A.; Belkoura, I.; Pliego-Alfaro, F.; Belkoura, M. Somatic Embryogenesis from Leaf and Petiole Explants of the Moroccan Olive Cultivar Dahbia. *Sci. Hortic.* **2012**, *159*, 88–95. [CrossRef]
12. Narváez, I.; Martín, C.; Jiménez-Díaz, R.M.; Mercado, J.A.; Pliego-Alfaro, F. Plant Regeneration via Somatic Embryogenesis in Mature Wild Olive Genotypes Resistant to the Defoliating Pathotype of *Verticillium dahliae*. *Front. Plant Sci.* **2019**, *10*, 1471. [CrossRef]
13. Cardoso, H.G.; Campos, M.C.; Pais, M.S.; Peixe, A. Somatic Embryogenesis in Iberian Grapevine (*Vitis vinifera*) Cultivars Using Carpels as Initial Explants: Protocol Establishment and Histological Evaluation. *J. Agric. Sci. Technol.* **2019**, *9*. [CrossRef]
14. Pires, R.; Cardoso, H.; Ribeiro, A.; Peixe, A.; Cordeiro, A. Somatic Embryogenesis from Mature Embryos of *Olea Europaea* L. Cv. 'Galega Vulgar' and Long-Term Management of Calli Morphogenic Capacity. *Plants* **2020**, *9*, 758. [CrossRef] [PubMed]
15. Sánchez-Romero, C. Somatic Embryogenesis in Olive. *Plants* **2021**, *10*, 433. [CrossRef]
16. Pritsa, T.S.; Voyiatzis, D.G. The in Vitro Morphogenetic Capacity of Olive Embryo Explants at Different Develop-mental Stages, as Affected by L-Glutamine, L-Arginine and 2,4-D. *J. Biol. Res.* **2004**, *1*, 55–61.
17. Mazri, M.A.; Naciri, R.; Belkoura, I. Maturation and Conversion of Somatic Embryos Derived from Seeds of Olive (*Olea Europaea* L.) Cv. Dahbia: Occurrence of Secondary Embryogenesis and Adventitious Bud Formation. *Plants* **2020**, *9*, 1489. [CrossRef]
18. Titouh, K.; Hadj Moussa, K.; Boufis, N.; Khelifi, L. Impact of Cultural Conditions on Germination of Olive (*Olea europaea* L.) Somatic Embryos and Plantlets Development from the Algerian Cultivar Chemlal. *Adv. Hortic. Sci.* **2022**, *36*, 185–191. [CrossRef]
19. Cerezo, S.; Mercado, J.A.; Pliego-Alfaro, F. An Efficient Regeneration System via Somatic Embryogenesis in Olive. *Plant Cell Tiss. Organ Cult.* **2011**, *106*, 337–344. [CrossRef]
20. Rugini, E.; Caricato, G. Somatic Embryogenesis and Plant Recovery from Mature Tissues of Olive Cultivars (*Olea europaea* L.) 'Canino' and 'Moraiolo'. *Plant Cell Rep.* **1995**, *14*, 257–260. [CrossRef]
21. Trabelsi, E.B.; Naija, S.; Elloumi, N.; Belfeleh, Z.; Msellem, M.; Ghezel, R.; Bouzid, S. Somatic Embryogenesis in Cell Suspension Cultures of Olive *Olea europaea* (L.) 'Chetoui'. *Acta Physiol. Plant* **2011**, *33*, 319–324. [CrossRef]
22. Toufik, I.; Guenoun, F.; Belkoura, I. Embryogenesis Expression from Somatic Explants of Olive (*Olea europaea* L.) Cv. Picual. *Moroc. J. Biol.* **2014**, *11*, 17–25.
23. Eigel, L.; Koop, H.-U. Nurse Culture of Individual Cells: Regeneration of Colonies from Single Protoplasts of *Nicotiana tabacum*, *Brassica napus* and *Hordeum vulgare*. *J. Plant Physiol.* **1989**, *134*, 577–581. [CrossRef]
24. Westcott, R.J. Production of Embryogenic Callus from Nonembryonic Explants of Norway Spruce Picea Abies (L.) Karst. *Plant Cell Rep.* **1994**, *14*, 47–49. [CrossRef]
25. Komai, F.; Morohashi, H.; Horita, M. Application of Nurse Culture for Plant Regeneration from Protoplasts of *Lilium japonicum* Thunb. *In Vitro Cell. Dev. Biol. Plant* **2006**, *42*, 252–255. [CrossRef]
26. Hargreaves, C.; Reeves, C.; Gough, K.; Montalbán, I.A.; Low, C.; Van Ballekom, S.; Dungey, H.S.; Moncaleán, P. Nurse Tissue for Embryo Rescue: Testing New Conifer Somatic Embryogenesis Methods in a F1 Hybrid Pine. *Trees* **2017**, *31*, 273–283. [CrossRef]
27. Dyachok, J.V.; Wiweger, M.; Kenne, L.; Von Arnold, S. Endogenous Nod-Factor-Like Signal Molecules Promote Early Somatic Embryo Development in Norway Spruce. *Plant Physiol.* **2002**, *128*, 523–533. [CrossRef]
28. Pernis, M.; Salaj, T.; Bellová, J.; Danchenko, M.; Baráth, P.; Klubicová, K. Secretome Analysis Revealed That Cell Wall Remodeling and Starch Catabolism Underlie the Early Stages of Somatic Embryogenesis in *Pinus nigra*. *Front. Plant Sci.* **2023**, *14*, 1225424. [CrossRef]
29. Nic-Can, G.I.; Galaz-Ávalos, R.M.; De-la-Peña, C.; Alcazar-Magaña, A.; Wrobel, K.; Loyola-Vargas, V.M. Somatic Embryogenesis: Identified Factors That Lead to Embryogenic Repression. A Case of Species of the Same Genus. *PLoS ONE* **2015**, *10*, e0126414. [CrossRef]
30. Awada, R.; Campa, C.; Gibault, E.; Déchamp, E.; Georget, F.; Lepelley, M.; Abdallah, C.; Erban, A.; Martinez-Seidel, F.; Kopka, J.; et al. Unravelling the Metabolic and Hormonal Machinery During Key Steps of Somatic Embryogenesis: A Case Study in Coffee. *Int. J. Mol. Sci.* **2019**, *20*, 4665. [CrossRef]
31. Awada, R.; Verdier, D.; Froger, S.; Brulard, E.; De Faria Maraschin, S.; Etienne, H.; Breton, D. An Innovative Automated Active Compound Screening System Allows High-Throughput Optimization of Somatic Embryogenesis in *Coffea arabica*. *Sci. Rep.* **2020**, *10*, 810. [CrossRef] [PubMed]
32. Ben-Amar, A. Secretome-Derived Cultured Cell System: Overview Towards Extracellular Protein Characterization and Biotechnological Applications. *J. Basic Appl. Sci.* **2021**, *17*, 13–24. [CrossRef]
33. Ngcala, M.G.; Goche, T.; Brown, A.P.; Chivasa, S.; Ngara, R. Heat Stress Triggers Differential Protein Accumulation in the Extracellular Matrix of Sorghum Cell Suspension Cultures. *Proteomes* **2020**, *8*, 29. [CrossRef] [PubMed]
34. Egertsdotter, U. Development of Somatic Embryos in Norway Spruce. *J. Exp. Bot.* **1998**, *49*, 155–162. [CrossRef]
35. Couillerot, J.-P.; Windels, D.; Vazquez, F.; Michalski, J.-C.; Hilbert, J.-L.; Blervacq, A.-S. Pretreatments, Condi-tioned Medium and Co-Culture Increase the Incidence of Somatic Embryogenesis of Different Cichorium Species. *Plant Sig. Behav* **2012**, *7*, 121–131. [CrossRef]

36. Guo, H.; Guo, H.; Zhang, L.; Tang, Z.; Yu, X.; Wu, J.; Zeng, F. Metabolome and Transcriptome Association Analysis Reveals Dynamic Regulation of Purine Metabolism and Flavonoid Synthesis in Transdifferentiation during Somatic Embryogenesis in Cotton. *Int. J. Mol. Sci.* **2019**, *20*, 2070. [CrossRef]
37. Gulzar, B.; Mujib, A.; Malik, M.Q.; Sayeed, R.; Mamgain, J.; Ejaz, B. Genes, Proteins and Other Networks Regu-lating Somatic Embryogenesis in Plants. *JGEB* **2020**, *18*, 31. [CrossRef]
38. Duchow, S.; Dahlke, R.I.; Geske, T.; Blaschek, W.; Classen, B. Arabinogalactan-Proteins Stimulate Somatic Embryogenesis and Plant Propagation of Pelargonium Sidoides. *Carbohydr. Polym.* **2016**, *152*, 149–155. [CrossRef]
39. Li, Z.; Zhang, D.; Shi, P.; Htwe, Y.M.; Yu, Q.; Huang, L.; Zhou, H.; Liu, L.; Wang, Y. Cell Wall Lignification May Be Necessary for Somatic Embryogenesis of Areca Palm (*Areca catechu*). *Sci. Hortic.* **2023**, *307*, 111538. [CrossRef]
40. Li, Q.; Zhang, S.; Wang, J. Transcriptomic and Proteomic Analyses of Embryogenic Tissues in *Picea balfouriana* Treated with 6-benzylaminopurine. *Physiol. Plant.* **2015**, *154*, 95–113. [CrossRef]
41. Fráterová, L.; Salaj, T.; Matušíková, I.; Salaj, J. The Role of Chitinases and Glucanases in Somatic Embryogenesis of Black Pine and Hybrid Firs. *Open Life Sci.* **2013**, *8*, 1172–1182. [CrossRef]
42. Kreuger, M.; Van Holst, G.-J. Arabinogalactan Proteins Are Essential in Somatic Embryogenesis of *Daucus carota* L. *Planta* **1993**, *189*, 243–248. [CrossRef]
43. Ben Amar, A.; Cobanov, P.; Ghorbel, A.; Mliki, A.; Reustle, G.M. Involvement of Arabinogalactan Proteins in the Control of Cell Proliferation of *Cucurbita pepo* Suspension Cultures. *Biol. Plant.* **2010**, *54*, 321–324. [CrossRef]
44. Tchorbadjieva, M.I. Protein Markers for Somatic Embryogenesis. In *Somatic Embryogenesis*; Mujib, A., Šamaj, J., Eds.; Plant Cell Monographs; Springer: Berlin/Heidelberg, Germany, 2006; Volume 2, pp. 215–233.
45. Rodríguez-Celma, J.; Ceballos-Laita, L.; Grusak, M.A.; Abadía, J.; López-Millán, A.-F. Plant Fluid Proteomics: Delving into the Xylem Sap, Phloem Sap and Apoplastic Fluid Proteomes. *Biophys. Acta Proteins Proteom.* **2016**, *1864*, 991–1002. [CrossRef]
46. Caeiro, A.; Ventura, F.; Correia, S.; Canhoto, J. Changes of Secondary Metabolites during Tamarillo Somatic Embryogenesis. *Biol. Life Sci. Forum* **2022**, *11*, 39. [CrossRef]
47. Segers, K.; Declerck, S.; Mangelings, D.; Heyden, Y.V.; Eeckhaut, A.V. Analytical Techniques for Metabolomic Studies: A Review. *Bioanalysis* **2019**, *11*, 2297–2318. [CrossRef]
48. Dowlatabadi, R.; Weljie, A.M.; Thorpe, T.A.; Yeung, E.C.; Vogel, H.J. Metabolic Footprinting Study of White Spruce Somatic Embryogenesis Using NMR Spectroscopy. *Plant Physiol. Biochem.* **2009**, *47*, 343–350. [CrossRef]
49. Cañas, L.A.; Benbadis, A. In Vitro Plant Regeneration from Cotyledon Fragments of the Olive Tree (*Olea europaea* L). *Plant Sci.* **1988**, *54*, 65–74. [CrossRef]
50. Orinos, T.; Mitrakos, K. Rhizogenesis and somatic embryogenesis in calli from wild olive (*Olea europaea* var. *sylvestris* (Miller) Lehr) mature zygotic embryos. *Plant Cell Tissue Organ Cult.* **1991**, *27*, 183–187. [CrossRef]
51. Regente, M.; Monzón, G.C.; De La Canal, L. Phospholipids Are Present in Extracellular Fluids of Imbibing Sunflower Seeds and Are Modulated by Hormonal Treatments. *J. Exp. Bot.* **2008**, *59*, 553–562. [CrossRef]
52. Genova, M.L.; Lenaz, G. Functional Role of Mitochondrial Respiratory Supercomplexes. *Biochim. Biophys. Acta* **2014**, *1837*, 427–443. [CrossRef] [PubMed]
53. Diniz, I.; Azinheira, H.; Figueiredo, A.; Gichuru, E.; Oliveira, H.; Guerra-Guimarães, L.; Silva, M.C. Fungal Penetration Associated with Recognition, Signaling and Defence-Related Genes and Peroxidase Activity during the Resistance Response of Coffee to *Colletotrichum kahawae*. *Physiol. Mol. Plant Pathol.* **2019**, *105*, 119–127. [CrossRef]
54. Loureiro, A.; Guerra-Guimarães, L.; Lidon, F.C.; Bertrand, B.; Silva, M.C.; Várzea, V. Isoenzymatic Characterization of *Colletotrichum kahawae* Isolates with Different Levels of Aggressiveness. *Trop. Plant Pathol.* **2011**, *36*, 287–293. [CrossRef]
55. Shaw, C.R.; Prasad, R. Starch gel electrophoresis of enzymes—A compilation of recipes. *Biochem. Genet.* **1970**, *4*, 297–320. [CrossRef]
56. Damerval, C.; De Vienne, D.; Zivy, M.; Thiellement, H. Technical Improvements in Two-dimensional Electrophoresis Increase the Level of Genetic Variation Detected in Wheat-seedling Proteins. *Electrophoresis* **1986**, *7*, 52–54. [CrossRef]
57. Wessel, D.; Flügge, U.I. A Method for the Quantitative Recovery of Protein in Dilute Solution in the Presence of Detergents and Lipids. *Anal. Biochem.* **1984**, *138*, 141–143. [CrossRef]
58. Laemmli, U. Cleavage of Structural Proteins during the Assembly of the Head of Bacteriophage T4. *Nature* **1970**, *227*, 680–685. [CrossRef]
59. Candiano, G.; Bruschi, M.; Musante, L.; Ghiggeri, G.M.; Carnemolla, B.; Orecchia, P.; Zardi, L.; Righetti, P.B. Blue Silver: A Very Sensitive Colloidal Coomassie G-250 Staining for Proteome Analysis. *Electrophoresis* **2004**, *25*, 1327–1333. [CrossRef]
60. Ciordia, S.; Alvarez-Sola, G.; Rullán, M.; Urman, J.M.; Ávila, M.A.; Corrales, F.J. Digging Deeper into Bile Proteome. *J. Proteom.* **2021**, *230*, 103984. [CrossRef]
61. Ciordia, S.; Alvarez-Sola, G.; Rullán, M.; Urman, J.M.; Ávila, M.A.; Corrales, F.J. Bile Processing Protocol for Improved Proteomic Analysis. In *Clinical Proteomics. Methods in Molecular Biology*; Humana: New York, NY, USA, 2022; Volume 2420.

62. Perez-Riverol, Y.; Bai, J.; Bandla, C.; García-Seisdedos, D.; Hewapathirana, S.; Kamatchinathan, S.; Kundu, D.J.; Prakash, A.; Frericks-Zipper, A.; Eisenacher, M.; et al. The PRIDE Database Resources in 2022: A Hub for Mass Spectrometry-Based Proteomics Evidences. *Nucleic Acids Res.* **2022**, *50*, D543–D552. [CrossRef]
63. Zhou, Y.; Zhou, B.; Pache, L.; Chang, M.; Khodabakhshi, A.H.; Tanaseichuk, O.; Benner, C.; Chanda, S.K. Metascape Provides a Biologist-Oriented Resource for the Analysis of Systems-Level Datasets. *Nat Commun.* **2019**, *10*, 1523. [CrossRef] [PubMed]
64. Gotz, S.; Garcia-Gomez, J.M.; Terol, J.; Williams, T.D.; Nagaraj, S.H.; Nueda, M.J.; Robles, M.; Talon, M.; Dopazo, J.; Conesa, A. High-Throughput Functional Annotation and Data Mining with the Blast2GO Suite. *Nucleic Acids Res.* **2008**, *36*, 3420–3435. [CrossRef]
65. Kanehisa, M.; Sato, Y.; Kawashima, M.; Furumichi, M.; Tanabe, M. KEGG as a Reference Resource for Gene and Protein Annotation. *Nucleic Acids Res.* **2016**, *44*, D457–D462. [CrossRef] [PubMed]
66. ElNaker, N.A.; Daou, M.; Ochsenkühn, M.A.; Amin, S.A.; Yousef, A.F.; Yousef, L.F. A Metabolomics Approach to Evaluate the Effect of Lyophilization versus Oven Drying on the Chemical Composition of Plant Extracts. *Sci. Rep.* **2021**, *11*, 22679. [CrossRef]
67. Rogulska, O.; Vackova, I.; Prazak, S.; Turnovcova, K.; Kubinova, S.; Bacakova, L.; Jendelova, P.; Petrenko, Y. Storage Conditions Affect the Composition of the Lyophilized Secretome of Multipotent Mesenchymal Stromal Cells. *Sci. Rep.* **2024**, *14*, 10243. [CrossRef]
68. Peng, W.; Chang, M.; Wu, Y.; Zhu, W.; Tong, L.; Zhang, G.; Wang, Q.; Liu, J.; Zhu, X.; Cheng, T.; et al. Lyophilized Powder of Mesenchymal Stem Cell Supernatant Attenuates Acute Lung Injury through the IL-6–p-STAT3–P63–JAG2 Pathway. *Stem Cell Res. Ther.* **2021**, *12*, 216. [CrossRef]
69. Abla, K.K.; Mehanna, M.M. Freeze-Drying: A Flourishing Strategy to Fabricate Stable Pharmaceutical and Biological Products. *Int. J. Pharm.* **2022**, *628*, 122233. [CrossRef] [PubMed]
70. Wu, X.; Gong, F.; Wang, F. Protein Extraction from Plant Tissues for 2DE and Its Application in Proteomic Analysis. *Proteomics* **2014**, *14*, 645–658. [CrossRef]
71. Shevchenko, A.; Tomas, H.; Havli, J.; Olsen, J.V.; Mann, M. In-Gel Digestion for Mass Spectrometric Characterization of Proteins and Proteomes. *Nat. Protoc.* **2006**, *1*, 2856–2860. [CrossRef]
72. Niu, L.; Zhang, H.; Wu, Z.; Wang, Y.; Liu, H.; Wu, X.; Wang, W. Modified TCA/Acetone Precipitation of Plant Proteins for Proteomic Analysis. *PLoS ONE* **2018**, *13*, e0202238. [CrossRef]
73. Zhang, Y.; Bottinelli, D.; Lisacek, F.; Luban, J.; Strambio-De-Castillia, C.; Varesio, E.; Hopfgartner, G. Optimization of Human Dendritic Cell Sample Preparation for Mass Spectrometry-Based Proteomic Studies. *Anal. Biochem.* **2015**, *484*, 40–50. [CrossRef] [PubMed]
74. Sharma, I.P.; Kumar, N.; Sharma, A.K. A Rapid Isolation Method of Extracellular Proteins Produced by Pseudomonad Strains. *App. Sci. Rep.* **2017**, *17*, 1–3. [CrossRef]
75. Saad, M.G.; Beyenal, H.; Dong, W.J. Dual Roles of the Conditional Extracellular Vesicles Derived from Pseudomonas Aeruginosa Biofilms: Promoting and Inhibiting Bacterial Biofilm Growth. *Biofilm* **2024**, *7*, 100183. [CrossRef] [PubMed]
76. Guerra-Guimarães, L.; Tenente, R.; Pinheiro, C.; Chaves, I.; Silva, M.D.C.; Cardoso, F.M.H.; Planchon, S.; Barros, D.R.; Renaut, J.; Ricardo, C.P. Proteomic Analysis of Apoplastic Fluid of *Coffea Arabica* Leaves Highlights Novel Biomarkers for Resistance against Hemileia Vastatrix. *Front. Plant Sci.* **2015**, *6*, 478. [CrossRef]
77. Jaswanthi, N.; Krishna, M.S.R.; Sahitya, U.L.; Suneetha, P. Apoplast Proteomic Analysis Reveals Drought Stress-Responsive Protein Datasets in Chilli (*Capsicum annuum* L.). *Data Brief* **2019**, *25*, 104041. [CrossRef]
78. Jiang, S.; Pan, L.; Zhou, Q.; Xu, W.; He, F.; Zhang, L.; Gao, H. Analysis of the Apoplast Fluid Proteome during the Induction of Systemic Acquired Resistance in *Arabidopsis thaliana*. *PeerJ* **2023**, *11*, e16324. [CrossRef]
79. Ribeiro, D.G.; De Almeida, R.F.; Fontes, W.; De Souza Castro, M.; De Sousa, M.V.; Ricart, C.A.O.; Da Cunha, R.N.V.; Lopes, R.; Scherwinski-Pereira, J.E.; Mehta, A. Stress and Cell Cycle Regulation during Somatic Embryogenesis Plays a Key Role in Oil Palm Callus Development. *J. Prot.* **2019**, *192*, 137–146. [CrossRef]
80. Peng, C.; Gao, F.; Tretyakova, I.N.; Nosov, A.M.; Shen, H.; Yang, L. Transcriptomic and Metabolomic Analysis of Korean Pine Cell Lines with Different Somatic Embryogenic Potential. *Int. J. Mol. Sci.* **2022**, *23*, 13301. [CrossRef]
81. Domżalska, L.; Kędracka-Krok, S.; Jankowska, U.; Grzyb, M.; Sobczak, M.; Rybczyński, J.J.; Mikuła, A. Proteomic Analysis of Stipe Explants Reveals Differentially Expressed Proteins Involved in Early Direct Somatic Embryogenesis of the Tree *Fern Cyathea Delgadii* Sternb. *Plant Sci.* **2017**, *258*, 61–76. [CrossRef]
82. Oulbi, S.; Kohaich, K.; Baaziz, M.; Belkoura, I.; Loutfi, K. Peroxidase Enzyme Fractions as Markers of Somatic Embryogenesis Capacities in Olive (*Olea europaea* L.). *Plants* **2021**, *10*, 901. [CrossRef]
83. Singh, A.K. Principles of Nanotoxicology. In *Engineered Nanoparticles*; Elsevier: Amsterdam, The Netherlands, 2016; pp. 171–227, ISBN 978-0-12-801406-6.
84. Kalluri, R.; LeBleu, V.S. The Biology, Function, and Biomedical Applications of Exosomes. *Science* **2020**, *367*, eaau6977. [CrossRef]
85. Tancini, B.; Buratta, S.; Delo, F.; Sagini, K.; Chiaradia, E.; Pellegrino, R.M.; Emiliani, C.; Urbanelli, L. Lysosomal Exocytosis: The Extracellular Role of an Intracellular Organelle. *Membranes* **2020**, *10*, 406. [CrossRef]

86. Ibata, K.; Yuzaki, M. Destroy the Old to Build the New: Activity-Dependent Lysosomal Exocytosis in Neurons. *Neurosci. Res.* **2021**, *167*, 38–46. [CrossRef]
87. Su, J.; Song, Y.; Zhu, Z.; Huang, X.; Fan, J.; Qiao, J.; Mao, F. Cell–Cell Communication: New Insights and Clinical Implications. *Sig. Transduct. Target Ther.* **2024**, *9*, 196. [CrossRef]
88. Morel, A.; Trontin, J.-F.; Corbineau, F.; Lomenech, A.-M.; Beaufour, M.; Reymond, I.; Le Metté, C.; Ader, K.; Harvengt, L.; Cadene, M.; et al. Cotyledonary Somatic Embryos of Pinus Pinaster Ait. Most Closely Resemble Fresh, Maturing Cotyledonary Zygotic Embryos: Biological, Carbohydrate and Proteomic Analyses. *Planta* **2014**, *240*, 1075–1095. [CrossRef]
89. Wang, F.-X.; Shang, G.-D.; Wu, L.-Y.; Xu, Z.-G.; Zhao, X.-Y.; Wang, J.-W. Chromatin Accessibility Dynamics and a Hierarchical Transcriptional Regulatory Network Structure for Plant Somatic Embryogenesis. *Dev. Cell* **2020**, *54*, 742–757.e8. [CrossRef] [PubMed]
90. Chaturvedi, U.C.; Shrivastava, R. Interaction of Viral Proteins with Metal Ions: Role in Maintaining the Structure and Functions of Viruses. *FEMS Immunol. Med. Microbiol.* **2005**, *43*, 105–114. [CrossRef] [PubMed]
91. Selvaraj, C.; Vijayalakshmi, P.; Alex, A.M.; Alothaim, A.S.; Vijayakumar, R.; Umapathy, V.R. Chapter Three—Metalloproteins Structural and Functional Insights into Immunological Patterns. In *Advances in Protein Chemistry and Structural Biology*; Academic Press: Cambridge, MA, USA, 2024.
92. Permyakov, E.A. Metal Binding Proteins. *Encyclopedia* **2021**, *1*, 261–292. [CrossRef]
93. Gallego, P.; Martin, L.; Blazquez, A.; Guerra, H.; Villalobos, N. Involvement of Peroxidase Activity in Developing Somatic Embryos of *Medicago Arborea* L. Identification of an Isozyme Peroxidase as Biochemical Marker of Somatic Embryogenesis. *J.Plant Physiol.* **2014**, *171*, 78–84. [CrossRef]
94. Arnholdt-Schmitt, B.; Ragonezi, C.; Cardoso, H. Do Mitochondria Play a Central Role in Stress-Induced Somatic Embryogenesis? In *In Vitro Embryogenesis in Higher Plants*; Germana, M.A., Lambardi, M., Eds.; Methods in Molecular Biology; Springer: New York, NY, USA, 2016; Volume 1359, pp. 87–100.
95. Belmonte, M.F.; Donald, G.; Reid, D.M.; Yeung, E.C.; Stasolla, C. Alterations of the Glutathione Redox State Improve Apical Meristem Structure and Somatic Embryo Quality in White Spruce (*Picea glauca*). *J. Exp. Bot.* **2005**, *56*, 2355–2364. [CrossRef]
96. Pasternak, T.; Potters, G.; Caubergs, R.; Jansen, M.A.K. Complementary Interactions between Oxidative Stress and Auxins Control Plant Growth Responses at Plant, Organ, and Cellular Level. *J. Experim. Bot.* **2005**, *56*, 1991–2001. [CrossRef] [PubMed]
97. Li, X.; Ahmad, S.; Ali, A.; Guo, C.; Li, H.; Yu, J.; Zhang, Y.; Gao, X.; Guo, Y. Characterization of Somatic Embryogenesis Receptor-Like Kinase 4 as a Negative Regulator of Leaf Senescence in Arabidopsis. *Cells* **2019**, *8*, 50. [CrossRef] [PubMed]
98. Zhang, H.; Zhou, J.; Kou, X.; Liu, Y.; Zhao, X.; Qin, G.; Wang, M.; Qian, G.; Li, W.; Huang, Y.; et al. Syntaxin of Plants71 Plays Essential Roles in Plant Development and Stress Response via Regulating pH Homeostasis. *Front. Plant Sci.* **2023**, *14*, 1198353. [CrossRef]
99. Dobrenel, T.; Marchive, C.; Azzopardi, M.; Clément, G.; Moreau, M.; Sormani, R.; Robaglia, C.; Meyer, C. Sugar Metabolism and the Plant Target of Rapamycin Kinase: A Sweet operaTOR? *Front. Plant Sci.* **2013**, *4*, 93. [CrossRef] [PubMed]
100. Ju, L.; Pan, Z.; Zhang, H.; Li, Q.; Liang, J.; Deng, G.; Yu, M.; Long, H. New Insights into the Origin and Evolution of α-Amylase Genes in Green Plants. *Sci. Rep.* **2019**, *9*, 4929. [CrossRef]
101. Damaris, R.N.; Lin, Z.; Yang, P.; He, D. The Rice Alpha-Amylase, Conserved Regulator of Seed Maturation and Germination. *Int. J. Mol. Sci.* **2019**, *20*, 450. [CrossRef]
102. Swaisgood, H.E. Characteristics of Milk. In *Fennema's Food Chemistry*; CRC Press: Boca Raton, FL, USA, 2007; pp. 885–921.
103. Simpson, J.P.; Olson, J.; Dilkes, B.; Chapple, C. Identification of the Tyrosine- and Phenylalanine-Derived Soluble Metabolomes of *Sorghum*. *Front. Plant Sci.* **2021**, *12*, 714164. [CrossRef]
104. Greenwell, Z.L.; Ruter, J.M. Effect of Glutamine and Arginine on Growth of Hibiscus Moscheutos "in Vitro". *Ornam. Hortic.* **2018**, *24*, 393–399. [CrossRef]
105. Okumoto, S.; Funck, D.; Trovato, M.; Forlani, G. Editorial: Amino Acids of the Glutamate Family: Functions beyond Primary Metabolism. *Front. Plant Sci.* **2016**, *7*, 318. [CrossRef]
106. Cruzat, V.; Macedo Rogero, M.; Noel Keane, K.; Curi, R.; Newsholme, P. Glutamine: Metabolism and Immune Function, Supplementation and Clinical Translation. *Nutrients* **2018**, *10*, 1564. [CrossRef]
107. Efzueni Rozali, S.; Rashid, K.A.; Mat Taha, R. Micropropagation of an Exotic Ornamental Plant, *Calathea crotalifera*, for Production of High Quality Plantlets. *Sci. World J.* **2014**, *2014*, 1–12. [CrossRef] [PubMed]
108. Lee, Y.J.; Hwang, K.S.; Choi, P.S. Effect of Carbon Sources on Somatic Embryogenesis and Cotyledon Number Variations in Carrot (*Daucus carota* L.). *J. Plant Biotechnol.* **2023**, *50*, 12. [CrossRef]
109. Wang, G.; Liu, Y.; Gao, Z.; Li, H.; Wang, J. Effects of Amino Acids on Callus Proliferation and Somatic Embryogenesis in *Litchi chinensis* Cv. 'Feizixiao'. *Horticulturae* **2023**, *9*, 1311. [CrossRef]
110. Bartos, P.M.C.; Gomes, H.T.; Do Amaral, L.I.V.; Teixeira, J.B.; Scherwinski-Pereira, J.E. Biochemical Events during Somatic Embryogenesis in *Coffea arabica* L. *3 Biotech* **2018**, *8*, 209. [CrossRef] [PubMed]

111. Pescador, R.; Kerbauy, G.B.; Kraus, J.E.; De Melo Ferreira, W.; Guerra, M.P.; Figueiredo-Ribeiro, R.D.C.L. Changes in Soluble Carbohydrates and Starch Amounts during Somatic and Zygotic Embryogenesis of *Acca sellowiana* (*Myrtaceae*). *Vitr. Cell. Dev. Biol. Plant* **2008**, *44*, 289–299. [CrossRef]
112. Xie, J.; Cai, K.; Hu, H.-X.; Jiang, Y.-L.; Yang, F.; Hu, P.; Cao, D.; Li, W.; Chen, Y.; Zhou, C.; et al. Structural Analysis of the CatalyticMechanism and Substrate Specificity of Anabaena Alkaline Invertase InvA Reveals a Novel Glucosidase. *J. Biol. Biol. Chem.* **2016**, *291*, 25667. [CrossRef]